HHS Public Access

Author manuscript

Sci Immunol. Author manuscript; available in PMC 2020 May 29.

Published in final edited form as:

Sci Immunol. 2019 November 29; 4(41): . doi:10.1126/sciimmunol.aax7965.

Chronic mucocutaneous candidiasis and connective tissue disorder in humans with impaired JNK1-dependent responses to IL-17A/F and TGF-β

Juan Li[1], **Marco Ritelli**[2], **Cindy S. Ma**[3,4], **Geetha Rao**[3,*], **Tanwir Habib**[5,*], **Emilie Corvilain**[6,7,*], **Salim Bougarn**[5,*], **Sophie Cypowyj**[1,*], **Lucie Grodecká**[8,*], **Romain Lévy**[6,7], **Vivien Béziat**[6,7], **Lei Shang**[1,†], **Kathryn Payne**[3], **Danielle T. Avery**[3], **Mélanie Migaud**[6,7], **Soraya Boucherit**[6,7], **Sabri Boughorbel**[5], **Andrea Guennoun**[5], **Maya Chrabieh**[6,7], **Franck Rapaport**[1], **Benedetta Bigio**[1], **Yuval Itan**[1,9,10], **Bertrand Boisson**[1,6,7], **Claire Fieschi**[11], **Valérie Cormier-Daire**[7,12], **Delfien Syx**[13], **Fransiska Malfait**[13], **Nicoletta Zoppi**[2], **Laurent Abel**[1,6,7,‡], **Tomáš Freiberger**[8,14,‡], **Harry C. Dietz**[15,16,‡], **Nico Marr**[5,17,‡], **Stuart G. Tangye**[3,4,‡], **Marina Colombi**[2,‡], **Jean-Laurent Casanova**[1,6,7,18,19,§,‖], **Anne Puel**[1,6,7,§,‖]

[1]St. Giles Laboratory of Human Genetics of Infectious Diseases, Rockefeller Branch, The Rockefeller University, New York, NY 10065, USA

[2]Division of Biology and Genetics, Department of Molecular and Translational Medicine, University of Brescia, 25123 Brescia, Italy, EU

[3]Immunology Division, Garvan Institute of Medical Research, Darlinghurst, New South Wales 2010, Australia

[4]St. Vincent's Clinical School, Faculty of Medicine, University of New South Wales, Sydney, New South Wales 2010, Australia

[5]Sidra Medicine, PO Box 26999, Doha, Qatar

[6]Laboratory of Human Genetics of Infectious Diseases, Necker Branch, INSERM U1163, Necker Hospital for Sick Children, 75015 Paris, France, EU

[7]Paris Descartes University, Imagine Institute, 75015 Paris, France, EU

[8]Molecular Genetics Laboratory, Centre for Cardiovascular Surgery and Transplantation, Brno 65691, Czech Republic, EU

[‖]Corresponding author. jean-laurent.casanova@rockefeller.edu (J-L.C.); anne.puel@inserm.fr (A.P.).
[*]These authors contributed equally to this work.
[†]Present address: Pfizer Emerging Science and Innovation, Cambridge, MA 02139, USA.
[‡]These authors contributed equally to this work.
[§]These authors contributed equally to this work.

Author contributions: J.L., M.R., C.S.M., G.R., S.C., L.G., R.L., V.B., K.P., D.T.A., M.M. and M. Chrabieh performed the experiments and analyzed the data. T.H., S. Bougarn, L.S., S. Boughorbel, A.G., F.R., and B. Bigio conducted WES, microarray, RNA-Seq, and computational analyses. E.C., M.M., and S. Boucherit provided clinical samples and analyzed clinical data. Y.I., B. Boisson, V.C.-D., D.S., F.M., N.Z., L.A., T.F., H.C.D., N.M., S.G.T., and M. Colombi provided expertise and feedback. J.L., J.-L.C., and A.P. designed the study and wrote the manuscript with the assistance of all coauthors.

Final version of paper: https://immunology.sciencemag.org/content/4/41/eaax7965.long

Competing interests: The authors declare that they have no competing interests.

Data and materials availability: The WES data are available from the Sequence Read Archive via accession number PRJNA563623. The microarray and RNA-Seq data have been deposited to the Gene Expression Omnibus and are accessible under accession number GSE137110.

[9]The Charles Bronfman Institute for Personalized Medicine, Icahn School of Medicine at Mount Sinai, New York, NY 10029, USA

[10]Department of Genetics and Genomic Sciences, Icahn School of Medicine at Mount Sinai, New York, NY 10029, USA

[11]Department of Clinical Immunology, Saint-Louis Hospital, Assistance Publique-Hôpitaux de Paris (AP-HP), 75010 Paris, France, EU

[12]Department of Medical Genetics, INSERM U1163, Necker Hospital for Sick Children, 75015 Paris, France, EU

[13]Center for Medical Genetics, Ghent University Hospital, 9000 Ghent, Belgium, EU

[14]Faculty of Medicine and Central European Institute of Technology, Masaryk University, Brno 62500, Czech Republic, EU

[15]McKusick-Nathans Institute of Genetic Medicine, Johns Hopkins University School of Medicine, Baltimore, MD 21205, USA

[16]Howard Hughes Medical Institute, Baltimore, MD 21205, USA

[17]College of Health and Life Sciences, Hamad Bin Khalifa University, PO Box 34110, Doha, Qatar

[18]Pediatric Hematology-Immunology Unit, Necker Hospital for Sick Children, 75015 Paris, France, EU

[19]Howard Hughes Medical Institute, New York, NY 10065, USA

Abstract

Genetic etiologies of chronic mucocutaneous candidiasis (CMC) disrupt human IL-17A/F-dependent immunity at mucosal surfaces, whereas those of connective tissue disorders (CTD) often impair the TGF-β-dependent homeostasis of connective tissues. The signaling pathways involved are incompletely understood. We report a three-generation family with an autosomal dominant (AD) combination of CMC and a novel CTD that clinically overlaps with Ehlers-Danlos syndrome (EDS). The patients are heterozygous for a private splice-site variant of *MAPK8*, the gene encoding c-Jun N-terminal kinase 1 (JNK1), a component of the MAPK signaling pathway. This variant is loss-of-expression and loss-of-function in the patients' fibroblasts, which display AD JNK1 deficiency by haploinsufficiency. These cells have impaired, but not abolished, responses to IL-17A and IL-17F. Moreover, the development of the patients' T_H17 cells was impaired *ex vivo* and *in vitro*, probably due to the involvement of JNK1 in the TGF-β-responsive pathway and further accounting for the patients' CMC. Consistently, the patients' fibroblasts displayed impaired JNK1- and c-Jun/ATF2-dependent induction of key extracellular matrix (ECM) components and regulators, but not of EDS-causing gene products, in response to TGF-β. Furthermore, they displayed a transcriptional pattern in response to TGF-β different from that of fibroblasts from patients with Loeys-Dietz syndrome and mutations of *TGFBR2* or *SMAD3*, further accounting for the patients' complex and unusual CTD phenotype. This experiment of Nature indicates that the integrity of the human JNK1-dependent MAPK signaling pathway is essential for IL-17A- and IL-17F-dependent mucocutaneous immunity to *Candida,* and for the TGF-β-dependent homeostasis of connective tissues.

Introduction

Chronic mucocutaneous candidiasis (CMC) is characterized by recurrent lesions of the skin, nails, oral and genital mucosae caused by *Candida albicans* (1). Patients with profound and broad inherited T-cell immunodeficiencies present CMC as one of their many infections (2). Most patients heterozygous for dominant-negative *STAT3* mutations (3) or gain-of-function *STAT1* mutations (4), and most patients with autosomal recessive (AR) RORγT (5) or ZNF341 deficiency (6, 7) present CMC among the infections suffered, the range of which is smaller than for patients with severe T-cell deficiencies. Patients with these various forms of syndromic CMC (SCMC) share a paucity of circulating T_H17 cells (5–13). Patients with AR AIRE deficiency display not only autoimmunity but also CMC as their only infection, due to the production of neutralizing autoantibodies against IL-17A and/or IL-17F (14, 15). Finally, isolated forms of CMC (ICMC), in which CMC is the predominant or only clinical manifestation in otherwise healthy individuals, can be due to autosomal dominant (AD) IL-17F deficiency, or inborn errors of the IL-17-responsive pathway, such as AR IL-17RA, IL-17RC, and ACT1 deficiencies (16–20). Fibroblasts and keratinocytes derived from these patients display impaired (AD IL-17F deficiency) (16) or abolished (AR IL-17RA, IL-17RC, or ACT1 deficiency) responses to IL-17A and IL-17F (16–19).

Patients with inherited ICMC do not, however, display any overt signs of connective tissue disorders (CTD), as their skin, joints, bones, and blood vessels are unaffected. Conversely, patients with CTDs, such as Ehlers-Danlos syndrome (EDS), Loeys-Dietz syndrome (LDS), and Marfan syndrome (MS), do not suffer from CMC (21). Whilst the genetic basis of hypermobile EDS (hEDS) is unknown (22), the other 13 subtypes of EDS are caused by various inborn errors of genes, many of which encode collagen or collagen-modifying enzymes (e.g. *COL1A1*, *COL1A2*, *COL3A1*, *COL5A1*, *COL5A2*, *ADAMTS2*, *PLOD1*) (22, 23). LDS is caused by inborn errors of the TGF-β signaling pathway (*TGFBR1*, *TGFBR2*, *SMAD2*, *SMAD3*, *TGFB2*, and *TGFB3*) (24), and MS by inborn errors of *FBN1,* which encodes fibrillin-1 (25). In these disorders, the homeostasis and integrity of connective tissues are impaired by dysfunctional extracellular matrix (ECM) proteins, the production of which is controlled by TGF-β in fibroblasts (24, 26).

Results

A private heterozygous *MAPK8* variant in a kindred with AD CMC and CTD

We studied three patients (P1, P2, and P3) from three generations of a French family with AD CMC and a CTD overlapping with hEDS (Fig. 1A; fig. S1A; table S1; and the “Case reports” section). We performed whole-exome sequencing (WES) and found no rare non-synonymous coding variants in any of the known CMC-, EDS-, LDS-, and MS-causing genes, all of which were well covered by WES (table S2). Under a complete penetrance model, we found 18 heterozygous non-synonymous variants common to the three patients and private to this family, i.e. not previously reported in the 1000 Genomes Project, the Single-Nucleotide Polymorphism Database, the NHLBI GO Exome Sequencing Project, the Exome Aggregation Consortium Genome Aggregation Database, the NHLBI’s TOPMed program (Bravo), or our in-house database of over 6,000 exomes from patients with various infectious diseases (fig. S1B and table S3). The most plausible candidate was a splice-site

mutation in the *MAPK8* gene, for which the biological distance to six of the eight known SCMC- and ICMC-causing genes other than *AIRE* (*IL17F*, *IL17RA*, *ACT1*, *STAT1*, *STAT3*, and *RORC*) was shortest in the human gene connectome (HGC), and the distance to the other two (*IL17RC* and *ZNF341*) ranked second-shortest (27, 28). The familial segregation of this private mutant *MAPK8* allele was consistent with a fully penetrant AD trait (Fig. 1, A and B). This nucleotide substitution (c.311+1G>A), one base pair downstream from exon IV (Fig. 1C), was predicted to affect splicing by altering the donor splice site (29). The c.311+1G>A mutation has a combined annotation-dependent depletion (CADD) score of 26 (30), which is above the mutation significance cutoff (MSC) threshold of 19.034 for *MAPK8* (31) (fig. S1C). Moreover, three of the four nonsense or frameshift mutations in *MAPK8* present in public databases have a minor allele frequency (MAF) $< 10^{-5}$, whereas the fourth, with a MAF of 0.0000114, has a CADD score below the MSC threshold (fig. S1C). Consistent with these findings, *MAPK8* has a gene damage index (GDI) of 0.32 (32), a neutrality index of 0.06 (33), and a SnIPRE *f* parameter of 0.329 (within the top 11% of genes within the genome subject to the greatest constraints) (34) (fig. S1D), indicating that this gene is highly conserved in human populations and has evolved under purifying selection. Finally, *MAPK8* has a probability of loss-of-function intolerance (pLI) score of 0.98, which is greater than the threshold of 0.9, above which genes are considered to be extremely intolerant to loss-of-function variants (35). The *MAPK8* mutation found in this kindred was therefore probably deleterious, with the potential to cause an AD disease.

A loss-of-expression mutant *MAPK8* allele

The *MAPK8* gene encodes JNK1, one of the three members of the JNK family. This protein is a component of the mitogen-activated protein kinase (MAPK) pathway that converts extracellular stimuli into cellular responses (36, 37). JNK1 is phosphorylated by upstream MAPK kinases (MAPKK), and in turn phosphorylates downstream activator protein-1 (AP-1) transcription factors, including c-Jun and ATF-2 (37). There are two long (JNK1α2 and JNK1β2, 54 kDa) and two short (JNK1α1 and JNK1β1, 46 kDa) isoforms, generated by alternative usage of exon VII or VIII and alternative splicing of exon XIII (38) (Fig. 1C). We amplified a cDNA fragment extending from exons III to V from Epstein-Barr virus (EBV)-transformed B cells and simian virus 40 (SV40)-transformed fibroblasts from the patients. In addition to the wild-type (WT) transcript (band 4), we detected four aberrant products (bands 1, 2, 3, and 5) (Fig. 2A). TA cloning and subsequent sequencing identified two aberrantly spliced transcripts: one in which intron IV was retained (band 2) and one in which exon IV was skipped (band 5) (Fig. 2A). Bands 1 and 3 were artifacts of heteroduplex formation (39). We then inserted a genomic fragment containing the WT or mutant intron IV together with the surrounding exons (IV and V) into an exon-trapping vector (Fig. 2B). The WT minigene was normally spliced, whereas the mutant minigene generated two aberrant splicing products; one in which exon IV was skipped and another in which intron IV was retained (Fig. 2B). This assay confirmed the direct impact of the c.311+1G>A mutation on *MAPK8* mRNA splicing, with no detectable leakiness. Both aberrant mRNAs were predicted to result in the creation of premature stop codons (Fig. 2C). Consistent with this prediction, the levels of WT *MAPK8* mRNA and JNK1 protein in the patients' cells were about half those in control cells (Fig. 2, D and E). Moreover, no truncated proteins were detected in the patients' cells (Fig. 2E) or in HEK293T cells transfected with the

corresponding mutant constructs, with or without the N-terminal Myc tag (Fig. 2F). The three patients were, therefore, heterozygous for a private loss-of-expression *MAPK8* allele.

Impaired IL-17A/F signaling in patients' fibroblasts

Human IL-17A, IL-17F, and IL-17A/F (referred to collectively as IL-17A/F) can activate JNK1 after binding to IL-17RA/IL-17RC, which is mostly expressed in various non-hematopoietic cells, thereby inducing the production of pro-inflammatory cytokines, chemokines, and antimicrobial peptides (40, 41). Upon stimulation with IL-17A/F, SV40-fibroblasts from the patients produced abnormally small amounts of growth-regulated oncogene-α (GRO-α) and IL-6, whereas SV40-fibroblasts from an IL-17RA-deficient patient did not respond at all (Fig. 3A). Similar results were obtained with primary fibroblasts (fig. S2A). The patients' cells had subnormal-to-normal responses to tumor necrosis factor-α (TNF-α) and IL-1β (Fig. 3B and fig. S2B). Moreover, the activation of AP-1 (c-Jun/ATF-2), unlike that of ERK1/2, p38, and NF-κB, was impaired in the patients' SV40-fibroblasts following stimulation with IL-17A, as shown by western blotting (fig. S2C). By contrast, AP-1 was normally activated by TNF-α and IL-1β (fig. S2D). Fibroblasts and leukocytes from the patients also responded normally to lymphotoxin α1β2 (LTα1β2) (IL-8 production) and Toll-like receptor (TLR) agonists (IL-6 and IL-8 production), respectively (fig. S2, E to G). Peripheral blood mononuclear cells (PBMCs) responded normally to IL-2 in combination with IL-17E (IL-5 production) (fig. S2H). Lentiviral transduction of the patients' SV40-fibroblasts with cDNAs encoding WT JNK1 isoforms, JNK1α1 and JNK1β1 in particular, but not with any of the mutant isoforms, restored the response to IL-17A (Fig. 3C and fig. S2I). This finding is consistent with the predominant protein expression of JNK1α1 and JNK1β1 in control SV40-fibroblasts (Fig. 2E). Moreover, the induction of GRO-α and IL-6 in control SV40-fibroblasts was not affected by the overexpression of any mutant JNK1 isoform, suggesting that the mutant allele is not dominant-negative (Fig. 3C and fig. S2I). This is consistent with the purifying selection exerted on the *MAPK8* locus (34) (fig. S1D). By contrast, the RNAi-mediated knockdown of *MAPK8* impaired the response to IL-17A in control fibroblasts (Fig. 3D and fig. S2, J and K). Finally, we performed RNA-Seq to delineate the range of IL-17A-responsive genes in primary fibroblasts. The number of upregulated or downregulated genes in response to IL-17A was much lower in the patients (fig. S2L). Several IL-17A/F target genes, including *CXCL1*, *CXCL2*, *IL6*, *IL8*, *C3*, and *ICAM1*, were less induced in the patients' cells (fig. S2M). Approximately 60% of IL-17RA/IL-17RC-dependent genes were JNK1-dependent (fig. S2N). Collectively, these findings indicate that heterozygosity for the private *MAPK8* c.311+1G>A loss-of-expression variant underlies a distinctive AD cellular phenotype, with impaired responses to IL-17A/F in fibroblasts, by haploinsufficiency. Moreover, impaired cellular responses to IL-17A/F in fibroblasts, and possibly in other cells, contribute to CMC (42, 43).

Low proportions of *ex vivo* or *in vitro* differentiated T_H17 cells

Given that mouse JNK1 is important for T-cell activation and differentiation (44–46), and that human TGF-β activates JNK1 (47) and is essential for T_H17 differentiation *in vitro* (48–50), we also investigated the development and function of T cells in the patients, testing the hypothesis that impaired T_H17 development in the patients might also contribute to their

CMC. The frequencies of naïve and CD45RA$^+$ effector memory (EMRA) CD4$^+$ and CD8$^+$ T cells in the patients were slightly higher, whereas those of central (CM) and effector memory (EM) CD4$^+$ and CD8$^+$ T cells were correspondingly slightly lower than those in healthy controls (Fig. 4A). The patients had higher proportions of T_H1 cells and lower proportions of T_H17 cells than controls, but normal proportions of the T_H2, T_H1*, T_{FH}, and T_{reg} subsets among circulating CD4$^+$ T cells, as shown by flow cytometry (51) (Fig. 4B). Normal amounts of IL-17A and IL-22 were secreted by whole blood stimulated with PMA plus ionomycin (Fig. 4C). *Ex vivo* memory CD4$^+$ T cells also expressed IL-17A and IL-17F, albeit in the lower part of the control range, and IFN-γ after stimulation with T-cell activation and expansion beads (TAE; anti-CD2/CD3/CD28 mAbs-conjugated beads) and PMA plus ionomycin (Fig. 4D). The patients' naïve CD4$^+$ T cells produced less IL-17A and IL-17F than control cells when cultured under T_H17-polarizing conditions (Fig. 4, E and F). This difference was more pronounced when memory CD4$^+$ T cells were tested under the same conditions (Fig. 4G). Finally, the percentages of transitional, naïve, and memory B cells, and of class-switched memory B cells were normal in these patients (fig. S3, A and B). The abilities of naïve and memory B cells to differentiate into antibody-secreting cells were also intact (fig. S3, C and D). Overall, the ability of T cells to produce IL-17A and IL-17F was 50% lower (*ex vivo*) and 75% lower (*in vitro*) in patients heterozygous for the *MAPK8* mutation. The *ex vivo* development of T_{reg} cells was largely unaffected, consistent with the absence of overt autoimmunity in the patients. The CMC in these patients is, thus, a combined consequence of lower proportions of T_H17 cells and impaired cellular responses to IL-17A/F. Both human IL-17A/F- and IL-17RA/IL-17RC-dependent mucocutaneous immunity to *C. albicans* are, therefore, dependent on JNK1.

Normal extracellular matrix organization but poor migratory capabilities of patients' fibroblasts

We subsequently investigated the pathogenesis of the novel and complex CTD phenotype of the patients. Previous studies have proposed an *in vitro* fibroblast phenotype common to most EDS patients, but apparently not observed in other inherited CTDs (52–55). This phenotype is characterized by generalized fibronectin-ECM (FN-ECM) disarray, low levels of expression of the canonical integrin receptor α5β1, and the recruitment of αvβ3 integrin (52–55). EDS fibroblasts also seem to display little or no type III collagen deposition in the ECM (COLLIII-ECM) and a variable disorganization of type V collagen (COLLV-ECM) (52–55). A specific myofibroblast-like phenotype of hEDS has also been proposed, based on the organization of α-smooth muscle actin (α-SMA), cadherin-11 (CAD-11) expression, and enhanced cell migration (56). Unlike cells from EDS patients, the primary fibroblasts of P2 displayed no FN-ECM disarray, and α5β1 integrin was organized as in control fibroblasts (Fig. 5A). Despite the low levels of COLLIII-ECM and a barely detectable organization of COLLV-ECM, P2's fibroblasts expressed the canonical collagen receptor, α2β1 integrin, normally, unlike EDS cells (Fig. 5A). The myofibroblast-specific markers α-SMA and CAD-11 were absent from the cells of P2, whereas they were present on hEDS fibroblasts (Fig. 5A). Consistent with this finding, the fibroblasts of P2 did not have the enhanced migratory capability reported for some hEDS fibroblasts, as shown by *in vitro* scratch and Transwell assays (Fig. 5, B and C). Instead, the fibroblasts of P2, like some cEDS cells, migrated poorly (Fig. 5, B and C), probably accounting for the poor wound healing observed

in the patients (see the “Case reports” section). Overall, these data suggest that, even though the clinical presentation in these patients overlaps with EDS, and despite the 2017 EDS diagnostic criteria for hEDS being met (22), the *in vitro* fibroblast phenotype of these patients is apparently different from that proposed for EDS in general, and for hEDS in particular (52–56).

Impaired TGF-β signaling in patients’ fibroblasts

We tested the hypothesis that the patients’ CTD resulted from dysfunctional TGF-β signaling, as this pathway controls the expression of key genes involved in the development and maintenance of the ECM (24). Upon TGF-β stimulation, the patients’ SV40-fibroblasts displayed impaired AP-1 (c-Jun/ATF-2) activation, whereas ERK1/2, p38, and SMAD2/3, were normally activated, as shown by western blotting (fig. S4A). Previous reports have suggested that TGF-β induces the expression of FN in a JNK1-dependent manner (57, 58). Consistent with these findings, the induction of FN production by TGF-β was impaired at both the mRNA and protein levels in the patients’ fibroblasts (Fig. 5D and fig. S4, B and C). The patients did not display spondylometaphyseal dysplasia (SMD), which can be caused by heterozygous *FN1* mutations (59), probably because their baseline FN-ECM organization levels were normal (Fig. 5A). By contrast, various SMAD2/3-dependent TGF-β target genes (58, 60), such as *COL1A1*, *COL1A2*, *COL3A1*, *COL5A1*, and *COL5A2,* encoding key components of the ECM and mutated in patients with cEDS and other forms of EDS (22), were normally induced by TGF-β in the patients’ cells (Fig. 5D and fig. S4, B and C). Finally, we performed a transcriptomic analysis of the cellular response to TGF-β in primary fibroblasts. The genome-wide transcriptional response to TGF-β was impaired in the patients’ cells (fig. S4D). A number of TGF-β-responsive genes, including *ELN*, *EDN1*, *IL11,* and *COMP* were not induced in the patients’ cells (Fig. 5E and fig. S4E). Consistently, their induction in control fibroblasts stimulated with TGF-β was impaired by the RNAi-mediated knockdown of *MAPK8* (Fig. 5, F and G and fig. S4F). These findings are consistent with previous reports of the presence of AP-1-binding motifs in the regulatory regions of *COMP* and *ELN* (61, 62), or of the AP-1-dependent induction of *EDN1* and *IL11* by TGF-β (63, 64). Mutations in these genes (59, 65–68) or in those encoding the corresponding receptors (69, 70) have already been reported in patients with various CTDs other than EDS, LDS, and MS (table S4). The study of the patients’ fibroblasts thus delineated the transcriptomic impact of impaired JNK1-dependent, SMAD2/3-independent TGF-β signaling. Moreover, fibroblasts from patients with LDS, heterozygous for mutations in *TGFBR2* or *SMAD3,* also showed impaired responses to TGF-β (fig. S4D), consistent with previous studies showing these mutations to be loss-of-function *in vitro* (71–73). However, their impact differed from that of JNK1 haploinsufficiency, as about 40% of JNK1-dependent genes were TGFBR2/SMAD3-independent (fig. S4G). This is consistent with the clinical differences observed between our patient’s particular CTD (displaying some overlap with hEDS) and LDS. In addition, about 30% of TGFBR2-dependent genes were SMAD3-independent (fig. S4H), potentially accounting for some of the phenotypic differences between LDS patients with *TGFBR2* and *SMAD3* mutations. Our findings provide a molecular and cellular basis for the complex new form of CTD displayed by the patients, with an impairment of the TGF-β-dependent induction of key ECM components

and regulators different from that of patients with another CTD, LDS, who are heterozygous for *TGFBR2* or *SMAD3* mutations.

Discussion

We have discovered a heterozygous loss-of-expression and loss-of-function mutation of *MAPK8* in a three-generation multiplex kindred with a rare combination of classic CMC and novel CTD (Fig. 6). Human JNK1 haploinsufficiency impairs IL-17A/F immunity in two ways, by reducing the responses of fibroblasts to IL-17RA/IL-17RC ligation and by compromising the TGF-β-dependent development of T_H17 cells, accounting for the impaired mucocutaneous immunity to *C. albicans* and subsequent development of CMC in these patients. These findings indicate that IL-17RA/IL-17RC-dependent protective mucocutaneous immunity to *C. albicans* is JNK1-dependent. We previously described CMC patients with biallelic mutations of *ACT1* (19). The findings reported here identify JNK1 as a key component of this antifungal pathway acting downstream from ACT1. They also indicate that haploinsufficiency at the *JNK1* locus has an impact on the development of T_H17 cells, probably due to the involvement of JNK1 in the TGF-β pathway.

Our data also suggest that JNK1 haploinsufficiency impairs the c-Jun/ATF-2-dependent, and SMAD2/3-independent, TGF-β-responsive pathway in fibroblasts, a novel cellular phenotype that probably accounts for the patients' complex and unusual CTD phenotype. Interestingly, the induction of collagen genes mutated in cEDS and other forms of EDS, such as *COL1A1* and *COL5A1*, was intact, whereas that of other ECM proteins, such as *COMP* and *ELN*, mutated in patients with other types of CTD (65, 66), was impaired. The impaired induction of genes encoding ECM regulators, such as *EDN1* and *IL11*, may also contribute to the patients' CTD phenotype. It is also relevant that the impact of heterozygous mutations of *MAPK8* differed from that of the *TGFBR2* or *SMAD3* of patients with LDS, in terms of the transcriptional response to TGF-β. Haploinsufficiency for JNK1 probably defines a novel CTD entity encompassing various clinical manifestations, some of which overlap with EDS, but not LDS. Cellular responses to cytokines other than IL-17A/F and TGF-β were apparently intact in cells from the patients. JNK1-deficient mice have defects of innate and adaptive immunity to various infections (74–76), but their connective tissues have not been studied. *MAPK8*-heterozygous mice have rarely been studied and seem to be normal (77). In conclusion, the integrity of the human JNK1 pathway is essential for IL-17A/F-dependent mucocutaneous immunity to *Candida* and for the TGF-β-dependent homeostasis of connective tissues.

Materials and Methods

Study design

We studied three patients from a kindred suffering from CMC and CTD. We analyzed this kindred by WES and found that the patients were heterozygous for a private splice-site mutation in *MAPK8*, the gene encoding JNK1. We evaluated the impact of this mutation in an overexpression system and in the patients' cells. We assessed the cellular responses to IL-17A/F and TGF-β of the patients' fibroblasts, the development and the differentiation properties of the patients' T and B cells.

Human subjects

The patients (P1, P2, and P3) were followed in their country of residence, France. Another family member (II.1) also participated to the genetic study. Informed consent was obtained from each patient, in accordance with local regulations and a protocol for research on human subjects approved by the institutional review board (IRB) of INSERM. Experiments were performed on samples from human subjects in the United States, France, Italy, and Australia, in accordance with local regulations and with the approval of the IRB of The Rockefeller University, the IRB of INSERM, the local ethical committee of Brescia, and the Sydney South West Area Health Service, respectively.

Whole-exome sequencing

Genomic DNA was extracted from whole blood and sheared with an S2 focused ultrasonicator (Covaris). An adaptor-ligated library was prepared with the TruSeq DNA Sample Prep Kit (Illumina). Exome capture was performed with the SureSelect Human All Exon V5 kit (Agilent Technologies). Paired-end sequencing was performed on a HiSeq 2500 System (Illumina) generating 100-base reads. The sequences were aligned with the GRCh37 build of the human genome reference sequence, with the Burrows-Wheeler Aligner (78). Downstream processing and variant calling were performed with the Genome Analysis Toolkit (79), SAMtools (80), and Picard tools (http://broadinstitute.github.io/picard/). All variants were annotated with in-house annotation software.

Cell culture and transfection

Primary fibroblasts were obtained from skin biopsy specimens and cultured in Dulbecco's modified Eagle medium (DMEM) (Gibco) supplemented with 10% fetal bovine serum (FBS) (Gibco). Peripheral blood mononuclear cells (PBMCs) were isolated from whole blood by density gradient centrifugation on Ficoll-Paque PLUS (GE Healthcare Life Sciences). Immortalized simian virus 40 (SV40)-transformed fibroblasts (SV40-fibroblasts) and Epstein-Barr virus (EBV)-transformed B (EBV-B) cells were generated as previously described (81). Human embryonic kidney 293T (HEK293T) (ATCC) and GP2-293 retroviral packaging cells (Clontech) were maintained in DMEM containing 10% FBS. HEK293T and GP2-293 cells were transiently transfected with the aid of X-tremeGENE 9 DNA Transfection Reagent (Roche). Primary fibroblasts were transfected with siRNA in the presence of Lipofectamine RNAiMAX Transfection Reagent (Thermo Fisher Scientific), in accordance with the manufacturer's instructions.

Molecular genetics

Genomic DNA was isolated from primary fibroblasts or EBV-B cells with the QIAamp DNA Mini Kit (QIAGEN). A fragment encompassing exon IV and intron IV of *MAPK8* was amplified by PCR with specific primers (table S5). The PCR products were analyzed by electrophoresis in 1% agarose gels and sequenced with the BigDye Terminator Cycle Sequencing Kit (Applied Biosystems). Sequencing products were purified by gel filtration on Sephadex G-50 Superfine columns (GE Healthcare Life Sciences) and sequences were analyzed in an ABI 3730 DNA Analyzer (Applied Biosystems).

Plasmids and siRNAs

JNK1α1 and *JNK1α2* were amplified from pCDNA3 FLAG JNK1α1 (Addgene) and pCDNA3 FLAG JNK1α2 (Addgene), respectively. *JNK1β1* and *JNK1β2* were amplified from the cDNA derived from SV40-fibroblasts. The full-length WT isoforms and truncated mutants were inserted into pTRIP-SFFV (82) and the pCMV6-AN-Myc-DDK tagged vector (OriGene), respectively. TA cloning and exon trapping were performed with the pCR4-TOPO vector (Thermo Fisher Scientific) and the pET01 vector (MoBiTec GmbH), respectively, according to the manufacturer's instructions. Control siRNA (D-001810-10) and *MAPK8* siRNA (L-003514-00) were obtained from Dharmacon.

Cell stimulation and cytokine production

SV40- and primary fibroblasts were plated on 24-well plates at a density of 6×10^4 cells per well, in 0.5 mL DMEM supplemented with 10% FBS. After 24 h, cells were left unstimulated or were stimulated with recombinant human (rh) IL-17A (317-ILB; R&D Systems), rh IL-17F (1335-IL; R&D Systems), rh IL-17A/F (5194-IL; R&D Systems), rh TNF-α (210-TA; R&D Systems), rh IL-1β (201-LB; R&D Systems), rh lymphotoxin α1/β2 (8884-LY; R&D Systems), LTA-SA (tlrl-slta; InvivoGen), Pam_3CSK_4 (tlrl-pms; InvivoGen), FSL-1 (tlrl-fsl; InvivoGen), Pam_2CSK_4 (tlrl-pm2s-1; InvivoGen), and lipopolysaccharide (LPS) (L9764; Sigma-Aldrich) for a further 24 h. ELISA kits were used to determine the levels of GRO-α (DY275; R&D Systems), IL-6 (88-7066; Invitrogen), and IL-8 (M9318; Sanquin) in the supernatants. SV40- and primary fibroblasts were cultured in DMEM supplemented with 1% FBS for 24 h and then stimulated with recombinant human TGF-β1 (240-B-002; R&D Systems) for various time periods. Protein levels were determined by ELISA for fibronectin (DY1918-05; R&D Systems), procollagen I (α1) (DY6220-05; R&D Systems), and IL-11 (DY218; R&D Systems). Whole blood was stimulated with IL-1β, Pam_3CSK_4, heat-killed *Staphylococcus aureus* (HKSA) (tlrl-hksa; InvivoGen), FSL-1, Pam_2CSK_4, LPS, R848 (tlrl-r848; InvivoGen), and PMA (P1585; Sigma-Aldrich) plus ionomycin (I3909; Sigma-Aldrich) for 24 h and IL-6 production was measured by ELISA. PBMCs were cultured in X-VIVO 15 (Lonza) containing 5% human serum AB (Lonza) and 100 ng/mL recombinant human thymic stromal lymphopoietin (TSLP) (1398-TS/CF; R&D Systems) for 24 h. Cells were washed and plated on 48-well plates, at a density of 4×10^6 cells per well, in 0.5 mL of X-VIVO 15 supplemented with 5% human serum AB in the presence of 10 ng/mL recombinant human IL-2 (202-IL; R&D Systems) and 10 ng/mL recombinant human IL-17E (1258-IL; R&D Systems). After 72 h, the amount of IL-5 present in each well was determined with an ELISA kit (DY205; R&D Systems).

Reverse transcription and PCR (RT-PCR)

Total RNA was extracted with the RNeasy Mini Kit (QIAGEN), according to the manufacturer's instructions. Reverse transcription was carried out with the SuperScript III First-Strand Synthesis System (Invitrogen). Conventional PCR was performed with the ChoiceTaq Blue DNA Polymerase (Denville Scientific) and the amplicons were analyzed by electrophoresis in 2% agarose gels. Quantitative PCR was performed with Fast SYBR Green Master Mix (Applied Biosystems) in the 7500 Fast Real-Time PCR System (Applied

Biosystems). The primer pairs used for conventional and quantitative PCR are listed in table S5.

Western blotting

Whole-cell lysates were prepared in RIPA buffer (50 mM Tris-HCl pH 7.5, 150 mM NaCl, 1% Nonidet P40, 0.5% sodium deoxycholate, and 0.1% SDS) supplemented with cOmplete Protease Inhibitor Cocktail (Roche). Proteins were separated by electrophoresis in either 10% Criterion XT Bis-Tris Protein Gels (Bio-Rad) or 4-20% Mini-PROTEAN TGX Precast Protein Gels (Bio-Rad) and the resulting bands were transferred onto Immobilon-P PVDF Membrane (Millipore). All blots were incubated overnight with primary antibodies and developed with the Pierce ECL Western Blotting Substrate (Thermo Scientific). The antibodies used in this study included antibodies (from Cell Signaling Technology) against JNK1 (3708), pc-Jun (2361), c-Jun (9165), pATF-2 (9221), ATF-2 (9226); pIκBα (9246), pp65 (3033), pp38 (9211), p38 (9212), pERK1/2 (4370), ERK1/2 (4695), pSMAD2 (3101), SMAD2 (5339), pSMAD3 (9520), SMAD3 (9523), SMAD4 (38454), Myc (2040); as well as IκBα (610690; BD Biosciences), p65 (sc-372; Santa Cruz Biotechnology), and β-actin (AM1829B; Abgent), and the following secondary antibodies: Amersham ECL Mouse IgG, HRP-linked whole Ab (from sheep) (NA931; GE Healthcare Life Sciences) and Amersham ECL Rabbit IgG, HRP-linked whole Ab (from donkey) (NA934; GE Healthcare Life Sciences).

Ex vivo T-cell activation

PBMCs were cultured in 48-well plates, at a density of 3×10^6 cells per mL, in RPMI 1640 medium (Gibco) containing 10% FBS with T-cell activation and expansion beads (TAE) (130-091-441; Miltenyi Biotec) or PMA plus ionomycin, in the presence of a protein transport inhibitor (GolgiPlug; BD Biosciences). After 12 h, the cells were collected and their expression of the indicated cytokines was assessed by flow cytometry, as previously described (17).

In vitro T-cell differentiation

Naïve and memory $CD4^+$ T cells were isolated and cultured under polarizing conditions, as previously described (6, 83). Briefly, cells were cultured with TAE beads alone (T_H0) or under T_H1 (IL-12 [20 ng/mL; R&D Systems]) or T_H17 (TGF-β1 [2.5 ng/mL; Peprotech], IL-1β [20 ng/mL; Peprotech], IL-6 [50 ng/mL; PeproTech], IL-21 [50 ng/mL; PeproTech], IL-23 [20 ng/mL; eBioscience]) polarizing conditions. After 5 d, the supernatants were harvested and the cells were restimulated with PMA/ionomycin for 6 h. The levels of specific cytokines were determined by intracellular staining and flow cytometry. The secretion of the indicated cytokines was determined with a cytometric bead array (BD Biosciences).

In vitro B-cell differentiation

Naïve and memory B cells were sorted and cultured in the presence of CD40L (200 ng/mL; R&D systems), with or without IL-21 (50 ng/mL; Peprotech) for 7 d, as previously

described (83). The production of IgA, IgG, and IgM was assessed by Ig heavy chain-specific ELISA (83).

Flow cytometry

Cells were surface-labeled with CD4-APC-Vio770 anti-human CD4 (clone M-T321; Miltenyi Biotec), Brilliant Violet 421 anti-human CD197 (CCR7) (clone G043H7; BioLegend), PE-CF594 anti-human CD45RA (clone HI100; BD Biosciences), and LIVE/DEAD™ Fixable Aqua Dead Cell Stain Kit (L34957; Thermo Fisher Scientific). Intracellular staining was performed with the Fixation/Permeabilization Solution Kit (BD Biosciences) and antibodies including Alexa Fluor 488 anti-IL-17A (clone eBio64DEC17; eBioscience), PE anti-IL-17F (clone SHLR17; eBioscience), and Alexa Fluor 700 anti-IFN-γ (clone 4S.B3; eBioscience). Samples were analyzed with a Gallios Flow Cytometer (Beckman Coulter) and FlowJo software.

Immunofluorescence microscopy

Primary fibroblasts were fixed with ice-cold methanol and incubated with antibodies against fibronectin (Sigma-Aldrich), type III collagen (Chemicon), and type V collagen (LifeSpan BioSciences) at a dilution of 1:100, and with anti-α-smooth muscle actin antibody (A2547; Sigma-Aldrich) at a concentration of 2 μg/mL, as previously described (52, 56, 84). For analysis of the α2β1, α5β1, and αvβ3 integrins, cells were fixed with 3% paraformaldehyde (PFA)/60 mM sucrose and permeabilized with 0.5% Triton X-100, as previously reported (84). In particular, cells were incubated with anti-α5β1 (MAB1969; Chemicon), anti-αvβ3 (MAB1976; Chemicon), and anti-α2β1 (MAB1998; Chemicon) integrin antibodies at a concentration of 4 μg/mL for 1 h. Cadherin-11 levels were investigated by fixing cells by incubation with 4% PFA/10 mM sucrose for 10 min, permeabilizing them by incubation with 0.1% Triton X-100 for 10 min, blocking them with by incubation with 2% BSA in PBS for 1 h, and then incubating them with anti-CDH11/cadherin OB antibody (Thermo Fisher Scientific) at a concentration of 2 μg/mL for 3 h, as previously described (56). The cells were washed and then stained with Alexa Fluor 488 anti-rabbit and Alexa Fluor 594 anti-mouse antibodies (Thermo Fisher Scientific), or with rhodamine-conjugated anti-goat IgG antibody (Chemicon) for 1 h. Immunofluorescence signals were acquired with a black-and-white CCD TV camera (SensiCam; PCO Computer Optics GmbH) mounted on a Zeiss Axiovert fluorescence microscope, and digitized with Image-Pro Plus software (Media Cybernetics).

In vitro scratch assay

Primary fibroblasts were plated on 35-mm Petri dishes at a density of 3×10^4 cells per dish and grown to confluence. The cell monolayers were wounded with a rubber policeman to generate an acellular area and dishes were marked to ensure the recording of the correct area. The monolayers were washed with PBS, rinsed in DMEM plus 10% FBS, and photographed with an inverted microscope at 0 and 48 h after scratching.

Transwell assay

Cell migration was evaluated in a Transwell assay with an 8 μm-pore filter (Corning Costar). Primary fibroblasts (5×10^4 cells) were resuspended in DMEM without FBS, placed in the upper chamber, and allowed to migrate for 6 h through the polycarbonate membrane into the bottom well, which was filled with DMEM containing 10% FBS. The cells that did not migrate were removed from the upper surface with a cotton swab. The cells that had migrated were collected in the bottom chamber. They were fixed in methanol, stained with the Diff-Quik staining kit (Medion Diagnostic GmbH), and quantified in 10 non-overlapping fields of 1 mm^2 with a light microscope.

Microarray and RNA-Seq analyses

Total RNA was extracted with the RNeasy Plus Micro Kit (QIAGEN), according to the manufacturer's instructions. Microarray analysis was performed with the GeneChip Human Gene 2.0 ST Array (Thermo Fisher Scientific). The raw expression data were normalized in R with the robust multi-array average (RMA) method (85) and the affy R package (86), and processed as previously described (87). RNA-Seq analysis was performed with TruSeq Stranded mRNA (Illumina) and standard polyA-based methods for library preparation. Paired-end sequencing with a read length of 150 bp and ~19 million reads per sample was carried out with a HiSeq 4000 system (Illumina). Raw reads were aligned to the human genome assembly (hg38) with STAR aligner (88). The number of reads mapping to each gene feature was determined with HTSeq (89). Differential expression was analyzed with an in-house script in R with DESeq2 (90) and ComplexHeatmap (91). In brief, fold changes in expression between non-stimulated and stimulated conditions were calculated for each individual and time point separately, and genes were further filtered based on a minimal 1.5-fold change in expression (upregulation or downregulation). The residual responses of the patients were calculated based on the number of responsive genes passing the above filter in both healthy controls (number of responsive genes in a subject / total number of responsive genes in healthy controls) × 100).

Statistical analysis

Unpaired *t* tests and two-tailed Mann-Whitney tests were used for comparisons of two groups. $P < 0.05$ was considered statistically significant in all tests performed with Prism software (GraphPad).

Supplementary Material

Refer to Web version on PubMed Central for supplementary material.

Acknowledgments:

We warmly thank the patients and their family for participating in the study. We thank R. Döffinger, J. Reichenbach, S. Dupuis-Girod, M. Beaudoin, A.-E. Fargeton and I. Meyts for their help searching for additional JNK1-deficient patients. We also thank all the members of the Laboratory of Human Genetics of Infectious Diseases for fruitful discussions and the members of the genomics core facility at Sidra Medicine for their contributions to Illumina library preparation and RNA sequencing.

Funding: This work was funded by the French National Research Agency (ANR) under the "Investments for the future" program (ANR-10-IAHU-01), the HGDIFD project (ANR-14-CE15-0006-01), the EURO-CMC project

(ANR-14-RARE-0005-02), the Integrative Biology of Emerging Infectious Diseases Laboratory of Excellence (ANR-10-LABX-62-IBEID), the *Institut National de la Santé et de la Recherche Médicale* (INSERM), Paris Descartes University, The Rockefeller University, Sidra Medicine, the Jeffrey Modell Foundation Translational Research Program, the Jeffrey Modell Centers Network, the St. Giles Foundation, the National Center for Research Resources of the National Institutes of Health (NIH), the National Center for Advancing Translational Sciences (NCATS) of the NIH (UL1TR001866), and the National Institute of Allergy and Infectious Diseases (NIAID) of the NIH (R01AI127564). C.S.M. was supported by an Early-Mid Career Research Fellowship from the Office of Health and Medical Research of the New South Wales State Government. T.F. and L.G. were supported by the Ministry of Health of the Czech Republic (16-34414A). D.S. and F.M. were supported by the Research Foundation Flanders (FWO) of Belgium. S.G.T. was supported by the National Health and Medical Research Council of Australia. A.P. was supported by an AP-HP transversal research contract.

References and Notes

1. Li J, Vinh DC, Casanova JL, Puel A, Inborn errors of immunity underlying fungal diseases in otherwise healthy individuals. Curr. Opin. Microbiol 40, 46–57 (2017). [PubMed: 29128761]
2. Puel A, Cypowyj S, Marodi L, Abel L, Picard C, Casanova JL, Inborn errors of human IL-17 immunity underlie chronic mucocutaneous candidiasis. Curr. Opin. Allergy Clin. Immunol 12, 616–622 (2012). [PubMed: 23026768]
3. Freeman AF, Holland SM, Clinical manifestations, etiology, and pathogenesis of the hyper-IgE syndromes. Pediatr. Res 65, 32R–37R (2009).
4. Toubiana J, Okada S, Hiller J, Oleastro M, Lagos Gomez M, Aldave Becerra JC, Ouachee-Chardin M, Fouyssac F, Girisha KM, Etzioni A, Van Montfrans J, Camcioglu Y, Kerns LA, Belohradsky B, Blanche S, Bousfiha A, Rodriguez-Gallego C, Meyts I, Kisand K, Reichenbach J, Renner ED, Rosenzweig S, Grimbacher B, van de Veerdonk FL, Traidl-Hoffmann C, Picard C, Marodi L, Morio T, Kobayashi M, Lilic D, Milner JD, Holland S, Casanova JL, Puel A, S. G.-o.-F. S. G. International, Heterozygous STAT1 gain-of-function mutations underlie an unexpectedly broad clinical phenotype. Blood 127, 3154–3164 (2016). [PubMed: 27114460]
5. Okada S, Markle JG, Deenick EK, Mele F, Averbuch D, Lagos M, Alzahrani M, Al-Muhsen S, Halwani R, Ma CS, Wong N, Soudais C, Henderson LA, Marzouqa H, Shamma J, Gonzalez M, Martinez-Barricarte R, Okada C, Avery DT, Latorre D, Deswarte C, Jabot-Hanin F, Torrado E, Fountain J, Belkadi A, Itan Y, Boisson B, Migaud M, Arlehamn CS, Sette A, Breton S, McCluskey J, Rossjohn J, de Villartay JP, Moshous D, Hambleton S, Latour S, Arkwright PD, Picard C, Lantz O, Engelhard D, Kobayashi M, Abel L, Cooper AM, Notarangelo LD, Boisson-Dupuis S, Puel A, Sallusto F, Bustamante J, Tangye SG, Casanova JL, IMMUNODEFICIENCIES. Impairment of immunity to Candida and Mycobacterium in humans with bi-allelic RORC mutations. Science 349, 606–613 (2015). [PubMed: 26160376]
6. Beziat V, Li J, Lin JX, Ma CS, Li P, Bousfiha A, Pellier I, Zoghi S, Baris S, Keles S, Gray P, Du N, Wang Y, Zerbib Y, Levy R, Leclercq T, About F, Lim AI, Rao G, Payne K, Pelham SJ, Avery DT, Deenick EK, Pillay B, Chou J, Guery R, Belkadi A, Guerin A, Migaud M, Rattina V, Ailal F, Benhsaien I, Bouaziz M, Habib T, Chaussabel D, Marr N, El-Benna J, Grimbacher B, Wargon O, Bustamante J, Boisson B, Muller-Fleckenstein I, Fleckenstein B, Chandesris MO, Titeux M, Fraitag S, Alyanakian MA, Leruez-Ville M, Picard C, Meyts I, Di Santo JP, Hovnanian A, Somer A, Ozen A, Rezaei N, Chatila TA, Abel L, Leonard WJ, Tangye SG, Puel A, Casanova JL, A recessive form of hyper-IgE syndrome by disruption of ZNF341-dependent STAT3 transcription and activity. Sci. Immunol 3, (2018).
7. Frey-Jakobs S, Hartberger JM, Fliegauf M, Bossen C, Wehmeyer ML, Neubauer JC, Bulashevska A, Proietti M, Frobel P, Noltner C, Yang L, Rojas-Restrepo J, Langer N, Winzer S, Engelhardt KR, Glocker C, Pfeifer D, Klein A, Schaffer AA, Lagovsky I, Lachover-Roth I, Beziat V, Puel A, Casanova JL, Fleckenstein B, Weidinger S, Kilic SS, Garty BZ, Etzioni A, Grimbacher B, ZNF341 controls STAT3 expression and thereby immunocompetence. Sci. Immunol 3, (2018).
8. Minegishi Y, Saito M, Tsuchiya S, Tsuge I, Takada H, Hara T, Kawamura N, Ariga T, Pasic S, Stojkovic O, Metin A, Karasuyama H, Dominant-negative mutations in the DNA-binding domain of STAT3 cause hyper-IgE syndrome. Nature 448, 1058–1062 (2007). [PubMed: 17676033]
9. de Beaucoudrey L, Puel A, Filipe-Santos O, Cobat A, Ghandil P, Chrabieh M, Feinberg J, von Bernuth H, Samarina A, Janniere L, Fieschi C, Stephan JL, Boileau C, Lyonnet S, Jondeau G, Cormier-Daire V, Le Merrer M, Hoarau C, Lebranchu Y, Lortholary O, Chandesris MO, Tron F,

Gambineri E, Bianchi L, Rodriguez-Gallego C, Zitnik SE, Vasconcelos J, Guedes M, Vitor AB, Marodi L, Chapel H, Reid B, Roifman C, Nadal D, Reichenbach J, Caragol I, Garty BZ, Dogu F, Camcioglu Y, Gulle S, Sanal O, Fischer A, Abel L, Stockinger B, Picard C, Casanova JL, Mutations in STAT3 and IL12RB1 impair the development of human IL-17-producing T cells. J. Exp. Med 205, 1543–1550 (2008). [PubMed: 18591412]

10. Ma CS, Chew GY, Simpson N, Priyadarshi A, Wong M, Grimbacher B, Fulcher DA, Tangye SG, Cook MC, Deficiency of Th17 cells in hyper IgE syndrome due to mutations in STAT3. J. Exp. Med 205, 1551–1557 (2008). [PubMed: 18591410]
11. Milner JD, Brenchley JM, Laurence A, Freeman AF, Hill BJ, Elias KM, Kanno Y, Spalding C, Elloumi HZ, Paulson ML, Davis J, Hsu A, Asher AI, O'Shea J, Holland SM, Paul WE, Douek DC, Impaired T(H)17 cell differentiation in subjects with autosomal dominant hyper-IgE syndrome. Nature 452, 773–776 (2008). [PubMed: 18337720]
12. Liu L, Okada S, Kong XF, Kreins AY, Cypowyj S, Abhyankar A, Toubiana J, Itan Y, Audry M, Nitschke P, Masson C, Toth B, Flatot J, Migaud M, Chrabieh M, Kochetkov T, Bolze A, Borghesi A, Toulon A, Hiller J, Eyerich S, Eyerich K, Gulacsy V, Chernyshova L, Chernyshov V, Bondarenko A, Grimaldo RM, Blancas-Galicia L, Beas IM, Roesler J, Magdorf K, Engelhard D, Thumerelle C, Burgel PR, Hoernes M, Drexel B, Seger R, Kusuma T, Jansson AF, Sawalle-Belohradsky J, Belohradsky B, Jouanguy E, Bustamante J, Bue M, Karin N, Wildbaum G, Bodemer C, Lortholary O, Fischer A, Blanche S, Al-Muhsen S, Reichenbach J, Kobayashi M, Rosales FE, Lozano CT, Kilic SS, Oleastro M, Etzioni A, Traidl-Hoffmann C, Renner ED, Abel L, Picard C, Marodi L, Boisson-Dupuis S, Puel A, Casanova JL, Gain-of-function human STAT1 mutations impair IL-17 immunity and underlie chronic mucocutaneous candidiasis. J. Exp. Med 208, 1635–1648 (2011). [PubMed: 21727188]
13. van de Veerdonk FL, Plantinga TS, Hoischen A, Smeekens SP, Joosten LA, Gilissen C, Arts P, Rosentul DC, Carmichael AJ, Smits-van der Graaf CA, Kullberg BJ, van der Meer JW, Lilic D, Veltman JA, Netea MG, STAT1 mutations in autosomal dominant chronic mucocutaneous candidiasis. N. Engl. J. Med 365, 54–61 (2011). [PubMed: 21714643]
14. Kisand K, Boe Wolff AS, Podkrajsek KT, Tserel L, Link M, Kisand KV, Ersvaer E, Perheentupa J, Erichsen MM, Bratanic N, Meloni A, Cetani F, Perniola R, Ergun-Longmire B, Maclaren N, Krohn KJ, Pura M, Schalke B, Strobel P, Leite MI, Battelino T, Husebye ES, Peterson P, Willcox N, Meager A, Chronic mucocutaneous candidiasis in APECED or thymoma patients correlates with autoimmunity to Th17-associated cytokines. J. Exp. Med 207, 299–308 (2010). [PubMed: 20123959]
15. Puel A, Doffinger R, Natividad A, Chrabieh M, Barcenas-Morales G, Picard C, Cobat A, Ouachee-Chardin M, Toulon A, Bustamante J, Al-Muhsen S, Al-Owain M, Arkwright PD, Costigan C, McConnell V, Cant AJ, Abinun M, Polak M, Bougneres PF, Kumararatne D, Marodi L, Nahum A, Roifman C, Blanche S, Fischer A, Bodemer C, Abel L, Lilic D, Casanova JL, Autoantibodies against IL-17A, IL-17F, and IL-22 in patients with chronic mucocutaneous candidiasis and autoimmune polyendocrine syndrome type I. J. Exp. Med 207, 291–297 (2010). [PubMed: 20123958]
16. Puel A, Cypowyj S, Bustamante J, Wright JF, Liu L, Lim HK, Migaud M, Israel L, Chrabieh M, Audry M, Gumbleton M, Toulon A, Bodemer C, El-Baghdadi J, Whitters M, Paradis T, Brooks J, Collins M, Wolfman NM, Al-Muhsen S, Galicchio M, Abel L, Picard C, Casanova JL, Chronic mucocutaneous candidiasis in humans with inborn errors of interleukin-17 immunity. Science 332, 65–68 (2011). [PubMed: 21350122]
17. Levy R, Okada S, Beziat V, Moriya K, Liu C, Chai LY, Migaud M, Hauck F, Al Ali A, Cyrus C, Vatte C, Patiroglu T, Unal E, Ferneiny M, Hyakuna N, Nepesov S, Oleastro M, Ikinciogullari A, Dogu F, Asano T, Ohara O, Yun L, Della Mina E, Bronnimann D, Itan Y, Gothe F, Bustamante J, Boisson-Dupuis S, Tahuil N, Aytekin C, Salhi A, Al Muhsen S, Kobayashi M, Toubiana J, Abel L, Li X, Camcioglu Y, Celmeli F, Klein C, AlKhater SA, Casanova JL, Puel A, Genetic, immunological, and clinical features of patients with bacterial and fungal infections due to inherited IL-17RA deficiency. Proc. Natl. Acad. Sci. U.S.A 113, E8277–E8285 (2016). [PubMed: 27930337]
18. Ling Y, Cypowyj S, Aytekin C, Galicchio M, Camcioglu Y, Nepesov S, Ikinciogullari A, Dogu F, Belkadi A, Levy R, Migaud M, Boisson B, Bolze A, Itan Y, Goudin N, Cottineau J, Picard C, Abel

L, Bustamante J, Casanova JL, Puel A, Inherited IL-17RC deficiency in patients with chronic mucocutaneous candidiasis. J. Exp. Med 212, 619–631 (2015). [PubMed: 25918342]

19. Boisson B, Wang C, Pedergnana V, Wu L, Cypowyj S, Rybojad M, Belkadi A, Picard C, Abel L, Fieschi C, Puel A, Li X, Casanova JL, An ACT1 mutation selectively abolishes interleukin-17 responses in humans with chronic mucocutaneous candidiasis. Immunity 39, 676–686 (2013). [PubMed: 24120361]
20. Bhattad S, Dinakar C, Pinnamaraju H, Ganapathy A, Mannan A, Chronic Mucocutaneous Candidiasis in an Adolescent Boy Due to a Novel Mutation in TRAF3IP2. J. Clin. Immunol 39, 596–599 (2019). [PubMed: 31292894]
21. Meester JAN, Verstraeten A, Schepers D, Alaerts M, Van Laer L, Loeys BL, Differences in manifestations of Marfan syndrome, Ehlers-Danlos syndrome, and Loeys-Dietz syndrome. Ann. Cardiothorac. Surg 6, 582–594 (2017). [PubMed: 29270370]
22. Malfait F, Francomano C, Byers P, Belmont J, Berglund B, Black J, Bloom L, Bowen JM, Brady AF, Burrows NP, Castori M, Cohen H, Colombi M, Demirdas S, De Backer J, De Paepe A, Fournel-Gigleux S, Frank M, Ghali N, Giunta C, Grahame R, Hakim A, Jeunemaitre X, Johnson D, Juul-Kristensen B, Kapferer-Seebacher I, Kazkaz H, Kosho T, Lavallee ME, Levy H, Mendoza-Londono R, Pepin M, Pope FM, Reinstein E, Robert L, Rohrbach M, Sanders L, Sobey GJ, Van Damme T, Vandersteen A, van Mourik C, Voermans N, Wheeldon N, Zschocke J, Tinkle B, The 2017 international classification of the Ehlers-Danlos syndromes. Am. J. Med. Genet. C Semin. Med. Genet 175, 8–26 (2017). [PubMed: 28306229]
23. Blackburn PR, Xu Z, Tumelty KE, Zhao RW, Monis WJ, Harris KG, Gass JM, Cousin MA, Boczek NJ, Mitkov MV, Cappel MA, Francomano CA, Parisi JE, Klee EW, Faqeih E, Alkuraya FS, Layne MD, McDonnell NB, Atwal PS, Bi-allelic Alterations in AEBP1 Lead to Defective Collagen Assembly and Connective Tissue Structure Resulting in a Variant of Ehlers-Danlos Syndrome. Am. J. Hum. Genet 102, 696–705 (2018). [PubMed: 29606302]
24. MacFarlane EG, Haupt J, Dietz HC, Shore EM, TGF-beta Family Signaling in Connective Tissue and Skeletal Diseases. Cold Spring Harb. Perspect. Biol 9, (2017).
25. Dietz HC, Cutting GR, Pyeritz RE, Maslen CL, Sakai LY, Corson GM, Puffenberger EG, Hamosh A, Nanthakumar EJ, Curristin SM, et al., Marfan syndrome caused by a recurrent de novo missense mutation in the fibrillin gene. Nature 352, 337–339 (1991). [PubMed: 1852208]
26. Verrecchia F, Mauviel A, Transforming growth factor-beta signaling through the Smad pathway: role in extracellular matrix gene expression and regulation. J. Invest. Dermatol 118, 211–215 (2002). [PubMed: 11841535]
27. Itan Y, Zhang SY, Vogt G, Abhyankar A, Herman M, Nitschke P, Fried D, Quintana-Murci L, Abel L, Casanova JL, The human gene connectome as a map of short cuts for morbid allele discovery. Proc. Natl. Acad. Sci. U.S.A 110, 5558–5563 (2013). [PubMed: 23509278]
28. Itan Y, Mazel M, Mazel B, Abhyankar A, Nitschke P, Quintana-Murci L, Boisson-Dupuis S, Boisson B, Abel L, Zhang SY, Casanova JL, HGCS: an online tool for prioritizing disease-causing gene variants by biological distance. BMC Genomics 15, 256 (2014). [PubMed: 24694260]
29. Desmet FO, Hamroun D, Lalande M, Collod-Beroud G, Claustres M, Beroud C, Human Splicing Finder: an online bioinformatics tool to predict splicing signals. Nucleic Acids Res 37, e67 (2009). [PubMed: 19339519]
30. Kircher M, Witten DM, Jain P, O'Roak BJ, Cooper GM, Shendure J, A general framework for estimating the relative pathogenicity of human genetic variants. Nat. Genet 46, 310–315 (2014). [PubMed: 24487276]
31. Itan Y, Shang L, Boisson B, Ciancanelli MJ, Markle JG, Martinez-Barricarte R, Scott E, Shah I, Stenson PD, Gleeson J, Cooper DN, Quintana-Murci L, Zhang SY, Abel L, Casanova JL, The mutation significance cutoff: gene-level thresholds for variant predictions. Nat. Methods 13, 109–110 (2016). [PubMed: 26820543]
32. Itan Y, Shang L, Boisson B, Patin E, Bolze A, Moncada-Velez M, Scott E, Ciancanelli MJ, Lafaille FG, Markle JG, Martinez-Barricarte R, de Jong SJ, Kong XF, Nitschke P, Belkadi A, Bustamante J, Puel A, Boisson-Dupuis S, Stenson PD, Gleeson JG, Cooper DN, Quintana-Murci L, Claverie JM, Zhang SY, Abel L, Casanova JL, The human gene damage index as a gene-level approach to prioritizing exome variants. Proc. Natl. Acad. Sci. U.S.A 112, 13615–13620 (2015). [PubMed: 26483451]

33. McDonald JH, Kreitman M, Adaptive protein evolution at the Adh locus in Drosophila. Nature 351, 652–654 (1991). [PubMed: 1904993]
34. Eilertson KE, Booth JG, Bustamante CD, SnIPRE: selection inference using a Poisson random effects model. PLoS Comput. Biol 8, e1002806 (2012). [PubMed: 23236270]
35. Lek M, Karczewski KJ, Minikel EV, Samocha KE, Banks E, Fennell T, O'Donnell-Luria AH, Ware JS, Hill AJ, Cummings BB, Tukiainen T, Birnbaum DP, Kosmicki JA, Duncan LE, Estrada K, Zhao F, Zou J, Pierce-Hoffman E, Berghout J, Cooper DN, Deflaux N, DePristo M, Do R, Flannick J, Fromer M, Gauthier L, Goldstein J, Gupta N, Howrigan D, Kiezun A, Kurki MI, Moonshine AL, Natarajan P, Orozco L, Peloso GM, Poplin R, Rivas MA, Ruano-Rubio V, Rose SA, Ruderfer DM, Shakir K, Stenson PD, Stevens C, Thomas BP, Tiao G, Tusie-Luna MT, Weisburd B, Won HH, Yu D, Altshuler DM, Ardissino D, Boehnke M, Danesh J, Donnelly S, Elosua R, Florez JC, Gabriel SB, Getz G, Glatt SJ, Hultman CM, Kathiresan S, Laakso M, McCarroll S, McCarthy MI, McGovern D, McPherson R, Neale BM, Palotie A, Purcell SM, Saleheen D, Scharf JM, Sklar P, Sullivan PF, Tuomilehto J, Tsuang MT, Watkins HC, Wilson JG, Daly MJ, MacArthur DG, Exome Aggregation C, Analysis of protein-coding genetic variation in 60,706 humans. Nature 536, 285–291 (2016). [PubMed: 27535533]
36. Johnson GL, Nakamura K, The c-jun kinase/stress-activated pathway: regulation, function and role in human disease. Biochim. Biophys. Acta 1773, 1341–1348 (2007). [PubMed: 17306896]
37. Hotamisligil GS, Davis RJ, Cell Signaling and Stress Responses. Cold Spring Harb. Perspect. Biol 8, (2016).
38. Manning AM, Davis RJ, Targeting JNK for therapeutic benefit: from junk to gold? Nat. Rev. Drug Discov 2, 554–565 (2003). [PubMed: 12815381]
39. Eckhart L, Ban J, Ballaun C, Weninger W, Tschachler E, Reverse transcription-polymerase chain reaction products of alternatively spliced mRNAs form DNA heteroduplexes and heteroduplex complexes. J. Biol. Chem 274, 2613–2615 (1999). [PubMed: 9915788]
40. Gaffen SL, Jain R, Garg AV, Cua DJ, The IL-23-IL-17 immune axis: from mechanisms to therapeutic testing. Nat. Rev. Immunol 14, 585–600 (2014). [PubMed: 25145755]
41. Li J, Casanova JL, Puel A, Mucocutaneous IL-17 immunity in mice and humans: host defense vs. excessive inflammation. Mucosal Immunol 11, 581–589 (2018). [PubMed: 29186107]
42. Puel A, Picard C, Cypowyj S, Lilic D, Abel L, Casanova JL, Inborn errors of mucocutaneous immunity to Candida albicans in humans: a role for IL-17 cytokines? Curr. Opin. Immunol 22, 467–474 (2010). [PubMed: 20674321]
43. Hernandez-Santos N, Gaffen SL, Th17 cells in immunity to Candida albicans. Cell Host Microbe 11, 425–435 (2012). [PubMed: 22607796]
44. Dong C, Yang DD, Wysk M, Whitmarsh AJ, Davis RJ, Flavell RA, Defective T cell differentiation in the absence of Jnk1. Science 282, 2092–2095 (1998). [PubMed: 9851932]
45. Conze D, Krahl T, Kennedy N, Weiss L, Lumsden J, Hess P, Flavell RA, Le Gros G, Davis RJ, Rincon M, c-Jun NH(2)-terminal kinase (JNK)1 and JNK2 have distinct roles in CD8(+) T cell activation. J. Exp. Med 195, 811–823 (2002). [PubMed: 11927626]
46. Ichiyama K, Sekiya T, Inoue N, Tamiya T, Kashiwagi I, Kimura A, Morita R, Muto G, Shichita T, Takahashi R, Yoshimura A, Transcription factor Smad-independent T helper 17 cell induction by transforming-growth factor-beta is mediated by suppression of eomesodermin. Immunity 34, 741–754 (2011). [PubMed: 21600798]
47. Zhang YE, Non-Smad Signaling Pathways of the TGF-beta Family. Cold Spring Harb. Perspect. Biol 9, (2017).
48. Manel N, Unutmaz D, Littman DR, The differentiation of human T(H)-17 cells requires transforming growth factor-beta and induction of the nuclear receptor RORgammat. Nat. Immunol 9, 641–649 (2008). [PubMed: 18454151]
49. Volpe E, Servant N, Zollinger R, Bogiatzi SI, Hupe P, Barillot E, Soumelis V, A critical function for transforming growth factor-beta, interleukin 23 and proinflammatory cytokines in driving and modulating human T(H)-17 responses. Nat. Immunol 9, 650–657 (2008). [PubMed: 18454150]
50. Yang L, Anderson DE, Baecher-Allan C, Hastings WD, Bettelli E, Oukka M, Kuchroo VK, Hafler DA, IL-21 and TGF-beta are required for differentiation of human T(H)17 cells. Nature 454, 350–352 (2008). [PubMed: 18469800]

51. Ma CS, Wong N, Rao G, Avery DT, Torpy J, Hambridge T, Bustamante J, Okada S, Stoddard JL, Deenick EK, Pelham SJ, Payne K, Boisson-Dupuis S, Puel A, Kobayashi M, Arkwright PD, Kilic SS, El Baghdadi J, Nonoyama S, Minegishi Y, Mahdaviani SA, Mansouri D, Bousfiha A, Blincoe AK, French MA, Hsu P, Campbell DE, Stormon MO, Wong M, Adelstein S, Smart JM, Fulcher DA, Cook MC, Phan TG, Stepensky P, Boztug K, Kansu A, Ikinciogullari A, Baumann U, Beier R, Roscioli T, Ziegler JB, Gray P, Picard C, Grimbacher B, Warnatz K, Holland SM, Casanova JL, Uzel G, Tangye SG, Monogenic mutations differentially affect the quantity and quality of T follicular helper cells in patients with human primary immunodeficiencies. J. Allergy Clin. Immunol 136, 993–1006 e1001 (2015). [PubMed: 26162572]
52. Chiarelli N, Carini G, Zoppi N, Dordoni C, Ritelli M, Venturini M, Castori M, Colombi M, Transcriptome-Wide Expression Profiling in Skin Fibroblasts of Patients with Joint Hypermobility Syndrome/Ehlers-Danlos Syndrome Hypermobility Type. PLoS One 11, e0161347 (2016). [PubMed: 27518164]
53. Zoppi N, Chiarelli N, Ritelli M, Colombi M, Multifaced Roles of the alphavbeta3 Integrin in Ehlers-Danlos and Arterial Tortuosity Syndromes' Dermal Fibroblasts. Int. J. Mol. Sci. 19, (2018).
54. Mendoza-Londono R, Chitayat D, Kahr WH, Hinek A, Blaser S, Dupuis L, Goh E, Badilla-Porras R, Howard A, Mittaz L, Superti-Furga A, Unger S, Nishimura G, Bonafe L, Extracellular matrix and platelet function in patients with musculocontractural Ehlers-Danlos syndrome caused by mutations in the CHST14 gene. Am. J. Med. Genet. A 158A, 1344–1354 (2012). [PubMed: 22581468]
55. Syx D, Van Damme T, Symoens S, Maiburg MC, van de Laar I, Morton J, Suri M, Del Campo M, Hausser I, Hermanns-Le T, De Paepe A, Malfait F, Genetic heterogeneity and clinical variability in musculocontractural Ehlers-Danlos syndrome caused by impaired dermatan sulfate biosynthesis. Hum. Mutat 36, 535–547 (2015). [PubMed: 25703627]
56. Zoppi N, Chiarelli N, Binetti S, Ritelli M, Colombi M, Dermal fibroblast-to-myofibroblast transition sustained by alphavss3 integrin-ILK-Snail1/Slug signaling is a common feature for hypermobile Ehlers-Danlos syndrome and hypermobility spectrum disorders. Biochim. Biophys. Acta 1864, 1010–1023 (2018).
57. Hocevar BA, Brown TL, Howe PH, TGF-beta induces fibronectin synthesis through a c-Jun N-terminal kinase-dependent, Smad4-independent pathway. EMBO J. 18, 1345–1356 (1999). [PubMed: 10064600]
58. Piek E, Ju WJ, Heyer J, Escalante-Alcalde D, Stewart CL, Weinstein M, Deng C, Kucherlapati R, Bottinger EP, Roberts AB, Functional characterization of transforming growth factor beta signaling in Smad2- and Smad3-deficient fibroblasts. J. Biol. Chem 276, 19945–19953 (2001). [PubMed: 11262418]
59. Lee CS, Fu H, Baratang N, Rousseau J, Kumra H, Sutton VR, Niceta M, Ciolfi A, Yamamoto G, Bertola D, Marcelis CL, Lugtenberg D, Bartuli A, Kim C, Hoover-Fong J, Sobreira N, Pauli R, Bacino C, Krakow D, Parboosingh J, Yap P, Kariminejad A, McDonald MT, Aracena MI, Lausch E, Unger S, Superti-Furga A, Lu JT, Baylor-Hopkins G Center for Mendelian, Cohn DH, Tartaglia M, Lee BH, Reinhardt DP, Campeau PM, Mutations in Fibronectin Cause a Subtype of Spondylometaphyseal Dysplasia with "Corner Fractures". Am. J. Hum. Genet 101, 815–823 (2017). [PubMed: 29100092]
60. Verrecchia F, Chu ML, Mauviel A, Identification of novel TGF-beta /Smad gene targets in dermal fibroblasts using a combined cDNA microarray/promoter transactivation approach. J. Biol. Chem 276, 17058–17062 (2001). [PubMed: 11279127]
61. Deere M, Rhoades Hall C, Gunning KB, LeFebvre V, Ridall AL, Hecht JT, Analysis of the promoter region of human cartilage oligomeric matrix protein (COMP). Matrix Biol. 19, 783–792 (2001). [PubMed: 11223338]
62. Oleggini R, Gastaldo N, Di Donato A, Regulation of elastin promoter by lysyl oxidase and growth factors: cross control of lysyl oxidase on TGF-beta1 effects. Matrix Biol. 26, 494–505 (2007). [PubMed: 17395448]
63. Shi-Wen X, Rodriguez-Pascual F, Lamas S, Holmes A, Howat S, Pearson JD, Dashwood MR, du Bois RM, Denton CP, Black CM, Abraham DJ, Leask A, Constitutive ALK5-independent c-Jun N-terminal kinase activation contributes to endothelin-1 overexpression in pulmonary fibrosis:

evidence of an autocrine endothelin loop operating through the endothelin A and B receptors. Mol. Cell. Biol 26, 5518–5527 (2006). [PubMed: 16809784]

64. Tang W, Yang L, Yang YC, Leng SX, Elias JA, Transforming growth factor-beta stimulates interleukin-11 transcription via complex activating protein-1-dependent pathways. J. Biol. Chem 273, 5506–5513 (1998). [PubMed: 9488674]
65. Briggs MD, Hoffman SM, King LM, Olsen AS, Mohrenweiser H, Leroy JG, Mortier GR, Rimoin DL, Lachman RS, Gaines ES, et al., Pseudoachondroplasia and multiple epiphyseal dysplasia due to mutations in the cartilage oligomeric matrix protein gene. Nat. Genet 10, 330–336 (1995). [PubMed: 7670472]
66. Zhang MC, He L, Giro M, Yong SL, Tiller GE, Davidson JM, Cutis laxa arising from frameshift mutations in exon 30 of the elastin gene (ELN). J. Biol. Chem 274, 981–986 (1999). [PubMed: 9873040]
67. Gordon CT, Petit F, Kroisel PM, Jakobsen L, Zechi-Ceide RM, Oufadem M, Bole-Feysot C, Pruvost S, Masson C, Tores F, Hieu T, Nitschke P, Lindholm P, Pellerin P, Guion-Almeida ML, Kokitsu-Nakata NM, Vendramini-Pittoli S, Munnich A, Lyonnet S, Holder-Espinasse M, Amiel J, Mutations in endothelin 1 cause recessive auriculocondylar syndrome and dominant isolated question-mark ears. Am. J. Hum. Genet 93, 1118–1125 (2013). [PubMed: 24268655]
68. Munroe PB, Olgunturk RO, Fryns JP, Van Maldergem L, Ziereisen F, Yuksel B, Gardiner RM, Chung E, Mutations in the gene encoding the human matrix Gla protein cause Keutel syndrome. Nat. Genet 21, 142–144 (1999). [PubMed: 9916809]
69. Gordon CT, Weaver KN, Zechi-Ceide RM, Madsen EC, Tavares AL, Oufadem M, Kurihara Y, Adameyko I, Picard A, Breton S, Pierrot S, Biosse-Duplan M, Voisin N, Masson C, Bole-Feysot C, Nitschke P, Delrue MA, Lacombe D, Guion-Almeida ML, Moura PP, Garib DG, Munnich A, Ernfors P, Hufnagel RB, Hopkin RJ, Kurihara H, Saal HM, Weaver DD, Katsanis N, Lyonnet S, Golzio C, Clouthier DE, Amiel J, Mutations in the endothelin receptor type A cause mandibulofacial dysostosis with alopecia. Am. J. Hum. Genet 96, 519–531 (2015). [PubMed: 25772936]
70. Nieminen P, Morgan NV, Fenwick AL, Parmanen S, Veistinen L, Mikkola ML, van der Spek PJ, Giraud A, Judd L, Arte S, Brueton LA, Wall SA, Mathijssen IM, Maher ER, Wilkie AO, Kreiborg S, Thesleff I, Inactivation of IL11 signaling causes craniosynostosis, delayed tooth eruption, and supernumerary teeth. Am. J. Hum. Genet 89, 67–81 (2011). [PubMed: 21741611]
71. van de Laar IM, Oldenburg RA, Pals G, Roos-Hesselink JW, de Graaf BM, Verhagen JM, Hoedemaekers YM, Willemsen R, Severijnen LA, Venselaar H, Vriend G, Pattynama PM, Collee M, Majoor-Krakauer D, Poldermans D, Frohn-Mulder IM, Micha D, Timmermans J, Hilhorst-Hofstee Y, Bierma-Zeinstra SM, Willems PJ, Kros JM, Oei EH, Oostra BA, Wessels MW, Bertoli-Avella AM, Mutations in SMAD3 cause a syndromic form of aortic aneurysms and dissections with early-onset osteoarthritis. Nat. Genet 43, 121–126 (2011). [PubMed: 21217753]
72. Lindsay ME, Schepers D, Bolar NA, Doyle JJ, Gallo E, Fert-Bober J, Kempers MJ, Fishman EK, Chen Y, Myers L, Bjeda D, Oswald G, Elias AF, Levy HP, Anderlid BM, Yang MH, Bongers EM, Timmermans J, Braverman AC, Canham N, Mortier GR, Brunner HG, Byers PH, Van Eyk J, Van Laer L, Dietz HC, Loeys BL, Loss-of-function mutations in TGFB2 cause a syndromic presentation of thoracic aortic aneurysm. Nat. Genet 44, 922–927 (2012). [PubMed: 22772368]
73. Meester JA, Vandeweyer G, Pintelon I, Lammens M, Van Hoorick L, De Belder S, Waitzman K, Young L, Markham LW, Vogt J, Richer J, Beauchesne LM, Unger S, Superti-Furga A, Prsa M, Dhillon R, Reyniers E, Dietz HC, Wuyts W, Mortier G, Verstraeten A, Van Laer L, Loeys BL, Loss-of-function mutations in the X-linked biglycan gene cause a severe syndromic form of thoracic aortic aneurysms and dissections. Genet. Med 19, 386–395 (2017). [PubMed: 27632686]
74. Rincon M, Davis RJ, Regulation of the immune response by stress-activated protein kinases. Immunol. Rev 228, 212–224 (2009). [PubMed: 19290930]
75. Van der Velden J, Janssen-Heininger YM, Mandalapu S, Scheller EV, Kolls JK, Alcorn JF, Differential requirement for c-Jun N-terminal kinase 1 in lung inflammation and host defense. PLoS One 7, e34638 (2012). [PubMed: 22514650]
76. Wang YQ, Ma X, Lu L, Zhao L, Zhang X, Xu Q, Wang Y, Defective antiviral CD8 T-cell response and viral clearance in the absence of c-Jun N-terminal kinases. Immunology 142, 603–613 (2014). [PubMed: 24673683]

77. Sabapathy K, Kallunki T, David JP, Graef I, Karin M, Wagner EF, c-Jun NH2-terminal kinase (JNK)1 and JNK2 have similar and stage-dependent roles in regulating T cell apoptosis and proliferation. J. Exp. Med 193, 317–328 (2001). [PubMed: 11157052]

78. Li H, Durbin R, Fast and accurate short read alignment with Burrows-Wheeler transform. Bioinformatics 25, 1754–1760 (2009). [PubMed: 19451168]

79. McKenna A, Hanna M, Banks E, Sivachenko A, Cibulskis K, Kernytsky A, Garimella K, Altshuler D, Gabriel S, Daly M, DePristo MA, The Genome Analysis Toolkit: a MapReduce framework for analyzing next-generation DNA sequencing data. Genome Res 20, 1297–1303 (2010). [PubMed: 20644199]

80. Li H, Handsaker B, Wysoker A, Fennell T, Ruan J, Homer N, Marth G, Abecasis G, Durbin R, Genome S Project Data Processing, The Sequence Alignment/Map format and SAMtools. Bioinformatics 25, 2078–2079 (2009). [PubMed: 19505943]

81. Zhang SY, Clark NE, Freije CA, Pauwels E, Taggart AJ, Okada S, Mandel H, Garcia P, Ciancanelli MJ, Biran A, Lafaille FG, Tsumura M, Cobat A, Luo J, Volpi S, Zimmer B, Sakata S, Dinis A, Ohara O, Garcia Reino EJ, Dobbs K, Hasek M, Holloway SP, McCammon K, Hussong SA, DeRosa N, Van Skike CE, Katolik A, Lorenzo L, Hyodo M, Faria E, Halwani R, Fukuhara R, Smith GA, Galvan V, Damha MJ, Al-Muhsen S, Itan Y, Boeke JD, Notarangelo LD, Studer L, Kobayashi M, Diogo L, Fairbrother WG, Abel L, Rosenberg BR, Hart PJ, Etzioni A, Casanova JL, Inborn Errors of RNA Lariat Metabolism in Humans with Brainstem Viral Infection. Cell 172, 952–965 e918 (2018). [PubMed: 29474921]

82. Lahaye X, Satoh T, Gentili M, Cerboni S, Silvin A, Conrad C, Ahmed-Belkacem A, Rodriguez EC, Guichou JF, Bosquet N, Piel M, Le Grand R, King MC, Pawlotsky JM, Manel N, Nuclear Envelope Protein SUN2 Promotes Cyclophilin-A-Dependent Steps of HIV Replication. Cell Rep. 15, 879–892 (2016). [PubMed: 27149839]

83. Ma CS, Wong N, Rao G, Nguyen A, Avery DT, Payne K, Torpy J, O'Young P, Deenick E, Bustamante J, Puel A, Okada S, Kobayashi M, Martinez-Barricarte R, Elliott M, Sebnem Kilic S, El Baghdadi J, Minegishi Y, Bousfiha A, Robertson N, Hambleton S, Arkwright PD, French M, Blincoe AK, Hsu P, Campbell DE, Stormon MO, Wong M, Adelstein S, Fulcher DA, Cook MC, Stepensky P, Boztug K, Beier R, Ikinciogullari A, Ziegler JB, Gray P, Picard C, Boisson-Dupuis S, Phan TG, Grimbacher B, Warnatz K, Holland SM, Uzel G, Casanova JL, Tangye SG, Unique and shared signaling pathways cooperate to regulate the differentiation of human CD4+ T cells into distinct effector subsets. J. Exp. Med 213, 1589–1608 (2016). [PubMed: 27401342]

84. Zoppi N, Gardella R, De Paepe A, Barlati S, Colombi M, Human fibroblasts with mutations in COL5A1 and COL3A1 genes do not organize collagens and fibronectin in the extracellular matrix, down-regulate alpha2beta1 integrin, and recruit alphavbeta3 Instead of alpha5beta1 integrin. J. Biol. Chem 279, 18157–18168 (2004). [PubMed: 14970208]

85. Irizarry RA, Hobbs B, Collin F, Beazer-Barclay YD, Antonellis KJ, Scherf U, Speed TP, Exploration, normalization, and summaries of high density oligonucleotide array probe level data. Biostatistics 4, 249–264 (2003). [PubMed: 12925520]

86. Gautier L, Cope L, Bolstad BM, Irizarry RA, affy--analysis of Affymetrix GeneChip data at the probe level. Bioinformatics 20, 307–315 (2004). [PubMed: 14960456]

87. Alsina L, Israelsson E, Altman MC, Dang KK, Ghandil P, Israel L, von Bernuth H, Baldwin N, Qin H, Jin Z, Banchereau R, Anguiano E, Ionan A, Abel L, Puel A, Picard C, Pascual V, Casanova JL, Chaussabel D, A narrow repertoire of transcriptional modules responsive to pyogenic bacteria is impaired in patients carrying loss-of-function mutations in MYD88 or IRAK4. Nat. Immunol 15, 1134–1142 (2014). [PubMed: 25344726]

88. Dobin A, Davis CA, Schlesinger F, Drenkow J, Zaleski C, Jha S, Batut P, Chaisson M, Gingeras TR, STAR: ultrafast universal RNA-seq aligner. Bioinformatics 29, 15–21 (2013). [PubMed: 23104886]

89. Anders S, Pyl PT, Huber W, HTSeq--a Python framework to work with high-throughput sequencing data. Bioinformatics 31, 166–169 (2015). [PubMed: 25260700]

90. Love MI, Huber W, Anders S, Moderated estimation of fold change and dispersion for RNA-seq data with DESeq2. Genome Biol. 15, 550 (2014). [PubMed: 25516281]

91. Gu Z, Eils R, Schlesner M, Complex heatmaps reveal patterns and correlations in multidimensional genomic data. Bioinformatics 32, 2847–2849 (2016). [PubMed: 27207943]

92. Smahi A, Courtois G, Vabres P, Yamaoka S, Heuertz S, Munnich A, Israel A, Heiss NS, Klauck SM, Kioschis P, Wiemann S, Poustka A, Esposito T, Bardaro T, Gianfrancesco F, Ciccodicola A, D'Urso M, Woffendin H, Jakins T, Donnai D, Stewart H, Kenwrick SJ, Aradhya S, Yamagata T, Levy M, Lewis RA, Nelson DL, Genomic rearrangement in NEMO impairs NF-kappaB activation and is a cause of incontinentia pigmenti. The International Incontinentia Pigmenti (IP) Consortium. Nature 405, 466–472 (2000). [PubMed: 10839543]

93. Ritelli M, Dordoni C, Venturini M, Chiarelli N, Quinzani S, Traversa M, Zoppi N, Vascellaro A, Wischmeijer A, Manfredini E, Garavelli L, Calzavara-Pinton P, Colombi M, Clinical and molecular characterization of 40 patients with classic Ehlers-Danlos syndrome: identification of 18 COL5A1 and 2 COL5A2 novel mutations. Orphanet J. Rare Dis 8, 58 (2013). [PubMed: 23587214]

94. von Bernuth H, Picard C, Jin Z, Pankla R, Xiao H, Ku CL, Chrabieh M, Mustapha IB, Ghandil P, Camcioglu Y, Vasconcelos J, Sirvent N, Guedes M, Vitor AB, Herrero-Mata MJ, Arostegui JI, Rodrigo C, Alsina L, Ruiz-Ortiz E, Juan M, Fortuny C, Yague J, Anton J, Pascal M, Chang HH, Janniere L, Rose Y, Garty BZ, Chapel H, Issekutz A, Marodi L, Rodriguez-Gallego C, Banchereau J, Abel L, Li X, Chaussabel D, Puel A, Casanova JL, Pyogenic bacterial infections in humans with MyD88 deficiency. Science 321, 691–696 (2008). [PubMed: 18669862]

95. van de Laar IM, van der Linde D, Oei EH, Bos PK, Bessems JH, Bierma-Zeinstra SM, van Meer BL, Pals G, Oldenburg RA, Bekkers JA, Moelker A, de Graaf BM, Matyas G, Frohn-Mulder IM, Timmermans J, Hilhorst-Hofstee Y, Cobben JM, Bruggenwirth HT, van Laer L, Loeys B, De Backer J, Coucke PJ, Dietz HC, Willems PJ, Oostra BA, De Paepe A, Roos-Hesselink JW, Bertoli-Avella AM, Wessels MW, Phenotypic spectrum of the SMAD3-related aneurysms-osteoarthritis syndrome. J. Med. Genet 49, 47–57 (2012). [PubMed: 22167769]

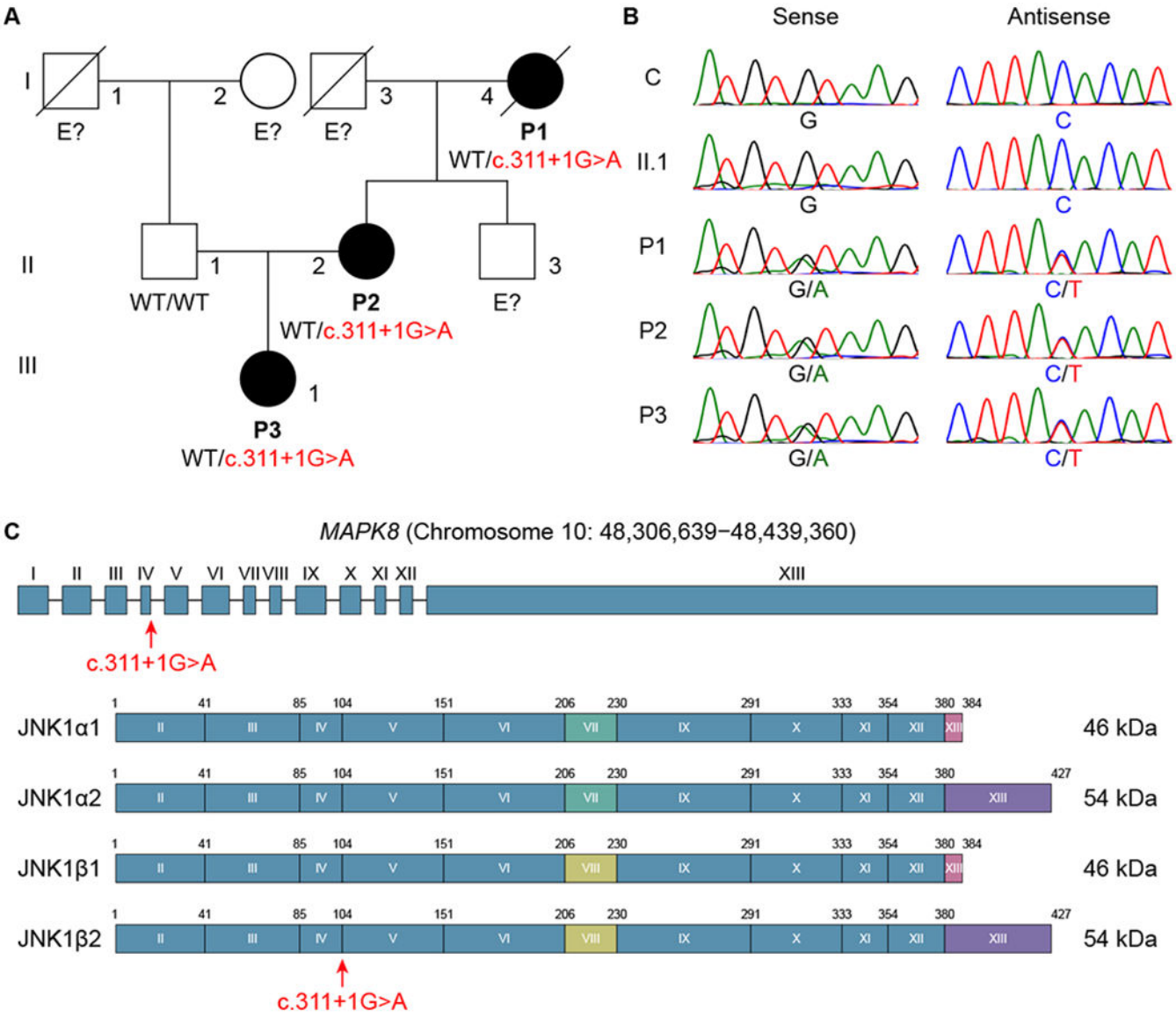

Fig. 1. Identification of a heterozygous *MAPK8* mutation in a kindred with AD CMC and CTD.

(**A**) Pedigree and segregation of the *MAPK8* mutation. The patients, in black, are heterozygous for the mutation. E? indicates individuals whose genetic status could not be evaluated. (**B**) Electropherograms of partial sequences of *MAPK8* corresponding to the mutation in a healthy control (C) and four members of the kindred (II.1, P1, P2, and P3). (**C**) Schematic illustration of the genomic locus and of the protein encoded by the *MAPK8* gene extracted from the Ensembl database. It has 13 exons (I-XIII), 12 of which are coding exons (II-XIII), encoding four isoforms (JNK1α1, JNK1α2, JNK1β1, and JNK1β2), with alternative usage of exon VII or VIII and alternative splicing of exon XIII. The red arrow indicates the position of the mutation.

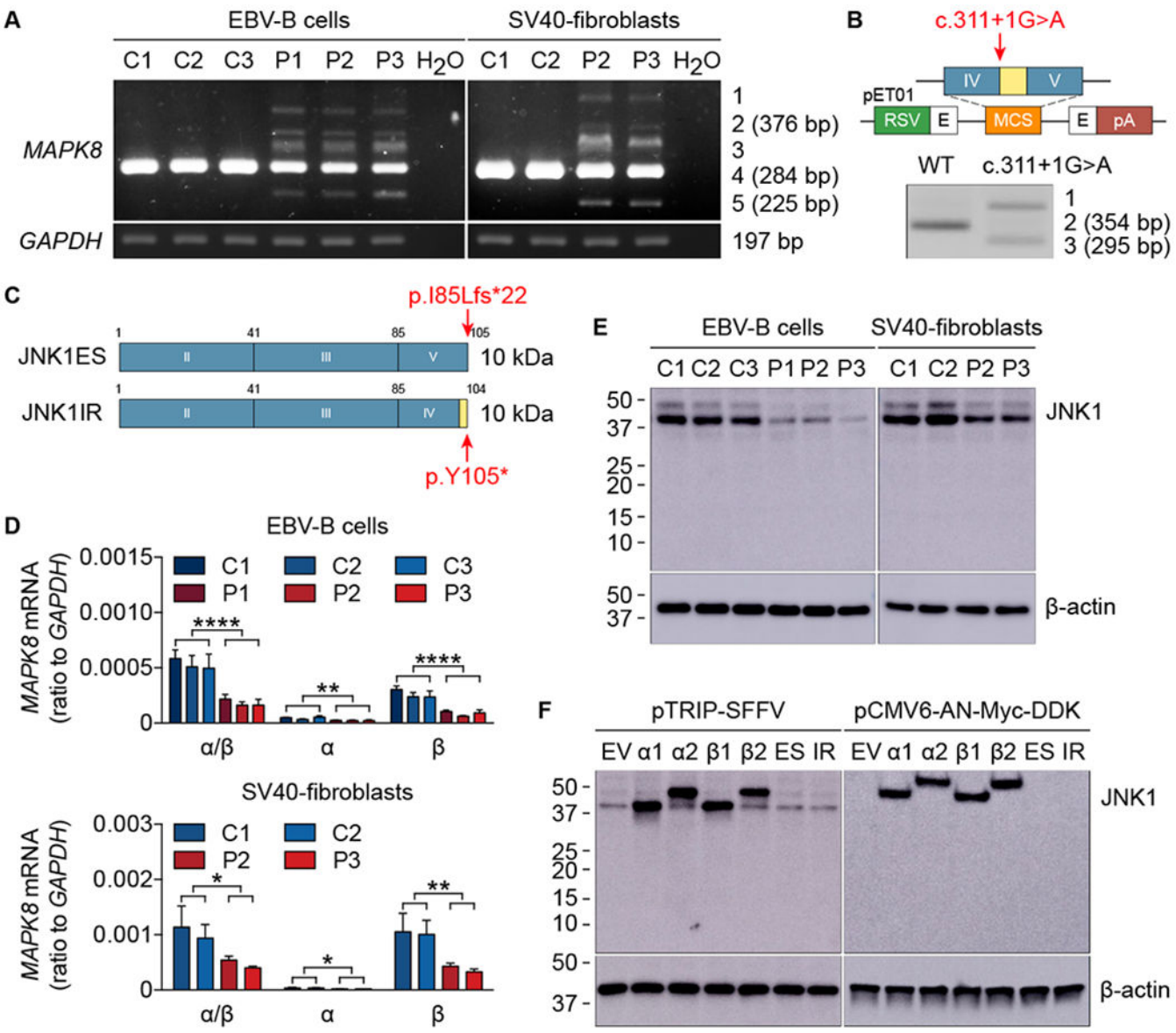

Fig. 2. The mutant *MAPK8* allele is loss-of-expression.

(**A**) *MAPK8* mRNA levels in EBV-B cells and SV40-fibroblasts from healthy controls (C1, C2, and C3) and patients (P1, P2, and P3). TA cloning and subsequent sequencing of the five bands generated by amplification from exon III to exon V identified three spliced transcripts: band 1 corresponding to the WT sequence together with intron IV retention and exon IV skipping; band 2 (376 bp) corresponding to intron IV retention; band 3 corresponding to the WT sequence together with exon IV skipping; band 4 (284 bp) corresponding to the WT sequence; band 5 (225 bp) corresponding to exon IV skipping. (**B**) Schematic diagram of the constructs used for exon trapping. pET01, exon-trapping vector; RSV, Rous sarcoma virus long terminal repeat promoter; pA, polyadenylation; E in black, exon of the pET01 vector; IV and V in blue, *MAPK8* exons IV and V; in yellow, *MAPK8* intron IV. The red arrow indicates the position of the mutation. RT-PCR and subsequent sequencing identified three spliced transcripts: band 1 corresponding to intron IV retention and exon IV skipping; band

2 (354 bp) corresponding to the WT sequence; band 3 (295 bp) corresponding to exon IV skipping. (**C**) Schematic illustration of the mutant proteins. JNK1ES (JNK1 exon skipping) represents exon IV skipping, whereas JNK1IR (JNK1 intron retention) denotes intron IV retention. Both transcripts are predicted to encode proteins of approximately 10 kDa in size. Red arrows indicate the positions of premature stop codons. (**D**) mRNA levels for *MAPK8* isoforms in EBV-B cells (top panel) and SV40-fibroblasts (bottom panel) from healthy controls (C1, C2, and C3) and patients (P1, P2, and P3). Quantitative RT-PCR was performed with primers specific for JNK1α1/JNK1α2 and JNK1β1/JNK1β2 mRNAs. α/β, total mRNA corresponding to JNK1α1, JNK1α2, JNK1β1, and JNK1β2; α, total mRNA corresponding to JNK1α1 and JNK1α2; β, total mRNA corresponding to JNK1β1 and JNK1β2. The values shown are the means ± SEM of three independent experiments. *, $P < 0.05$, **, $P < 0.01$, and ****, $P < 0.0001$; in unpaired *t* tests. (**E** and **F**) Immunoblot of JNK1 in EBV-B cells and SV40-fibroblasts from healthy controls (C1, C2, and C3) and patients (P1, P2, and P3) (**E**), and in HEK293T cells transfected with plasmids encoding four WT JNK1 isoforms (α1, α2, β1, and β2) and two mutants (ES and IR) inserted into the pTRIP-SFFV vector or the pCMV6-AN-Myc-DDK vector (**F**). Endogenous JNK1 was detected with an anti-JNK1 antibody recognizing the N-terminus of JNK1. Myc-tagged JNK1 was detected with an anti-Myc antibody. EV, empty vector. The data shown are representative of three independent experiments (**A**, **B**, **E**, and **F**).

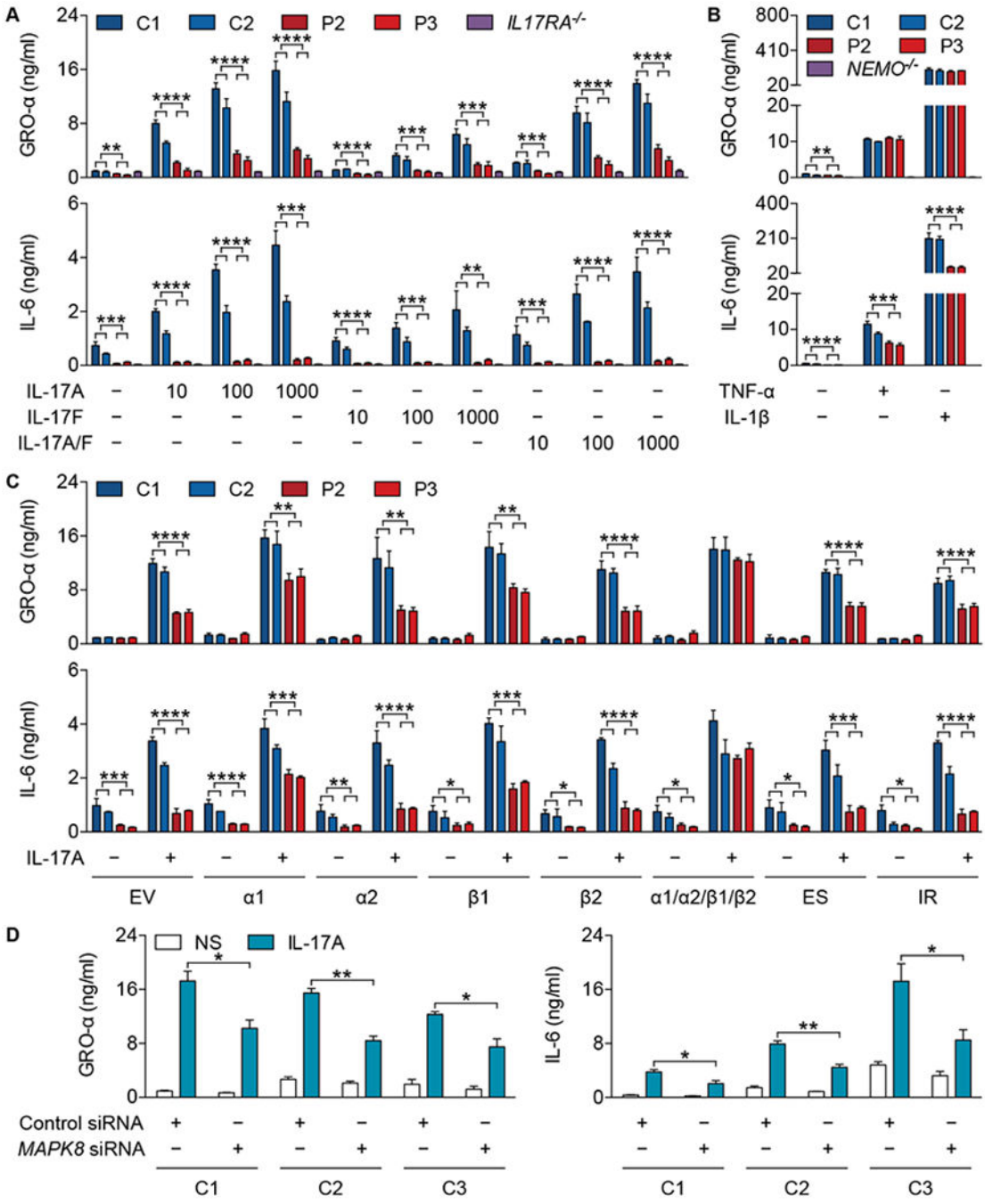

Fig. 3. The *MAPK8* variant impairs fibroblast responses to IL-17A/F.

(**A**) Production of GRO-α (top panel) and IL-6 (bottom panel) by SV40-fibroblasts from healthy controls (C1 and C2), patients (P2 and P3), and an IL-17RA-deficient (*IL17RA*$^{-/-}$) patient (16) stimulated with IL-17A, IL-17F, or IL-17A/F (10, 100, or 1000 ng/mL) for 24 h. (**B**) Production of GRO-α (top panel) and IL-6 (bottom panel) by SV40-fibroblasts from healthy controls (C1 and C2), patients (P2 and P3), and a NEMO-deficient (*NEMO*$^{-/-}$) patient (92) stimulated with TNF-α (20 ng/mL) or IL-1β (10 ng/mL) for 24 h. (**C**) Production of GRO-α (top panel) and IL-6 (bottom panel) by SV40-fibroblasts from healthy

controls (C1 and C2) and patients (P2 and P3) transfected with empty vector (EV) or plasmids encoding WT JNK1α1 (α1), JNK1α2 (α2), JNK1β1 (β1), JNK1β2 (β2), all four isoforms (α1/α2/β1/β2), JNK1ES (ES), or JNK1IR (IR), in the presence of IL-17A (100 ng/mL), for 24 h. (**D**) Production of GRO-α (left panel) and IL-6 (right panel) by primary fibroblasts from healthy controls (C1, C2, and C3) transfected with control siRNA (50 nM) or *MAPK8* siRNA (50 nM) for 24 h and then stimulated with IL-17A (100 ng/mL) for an additional 24 h. The values shown are the means ± SEM of three independent experiments (**A**-**D**). *, $P < 0.05$, **, $P < 0.01$, ***, $P < 0.001$, and ****, $P < 0.0001$; in unpaired *t* tests (**A**-**D**).

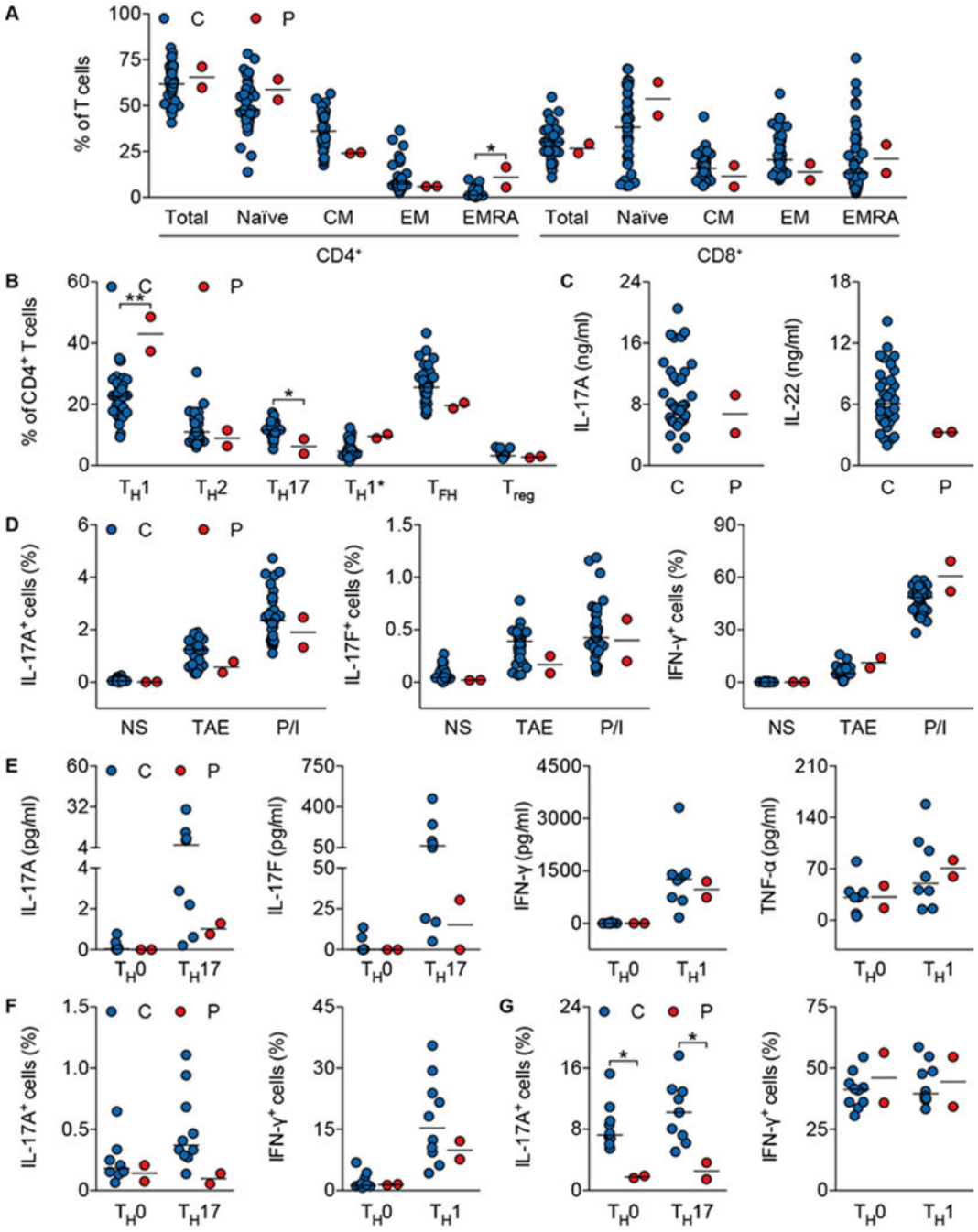

Fig. 4. Compromised T-cell differentiation in the patients.

(**A**) Percentage of total, naïve ($CCR7^+CD45RA^+$), central memory (CM; $CCR7^+CD45RA^-$), effector memory (EM; $CCR7^-CD45RA^-$), or $CD45RA^+$ effector memory (EMRA; $CCR7^-CD45RA^+$) $CD4^+$ and $CD8^+$ T cells from healthy controls (n=40) and patients (P2 and P3). (**B**) Frequency of T_H1 ($CXCR5^-CXCR3^+CCR6^-$), T_H2 ($CXCR5^-CXCR3^-CCR6^-CCR4^+$), T_H17 ($CXCR5^-CXCR3^-CCR6^+CCR4^+$), T_H1^* ($CXCR5^-CXCR3^+CCR6^+CCR4^+$), T_{FH} ($CXCR5^+$), and T_{reg} ($CD25^+FOXP3^+$) subsets among $CD4^+$ T cells from healthy controls (T_H1, T_H2, T_H17, T_H1^*, and T_{FH}, n=34; T_{reg},

n=17) and patients (P2 and P3). (**C**) Production of IL-17A and IL-22 by whole blood from healthy controls (*n*=33) and patients (P2 and P3) after stimulation with PMA plus ionomycin for 24 h. (**D**) Percentage of IL-17A$^+$, IL-17F$^+$, and IFN-γ^+ cells among memory CD4$^+$ T cells from healthy controls (*n*=36) and patients (P2 and P3) activated by T-cell activation and expansion (TAE) beads or PMA plus ionomycin (P/I) for 12 h. (**E**) Cytokine production by naïve CD4$^+$ T cells from healthy controls (*n*=8) and patients (P2 and P3) cultured under T_H0-, T_H17- or T_H1-polarizing conditions. (**F** and **G**) Frequency of IL-17A$^+$ and IFN-γ^+ cells among naïve (**F**) and memory (**G**) CD4$^+$ T cells from healthy controls (*n*=10) and patients (P2 and P3) cultured under T_H0-, T_H17- or T_H1-polarizing conditions. C, Healthy controls; P, P2 and P3. Horizontal bars represent median values (**A-G)**. *, $P < 0.05$ and **, $P < 0.01$; in two-tailed Mann-Whitney tests (**A-G)**.

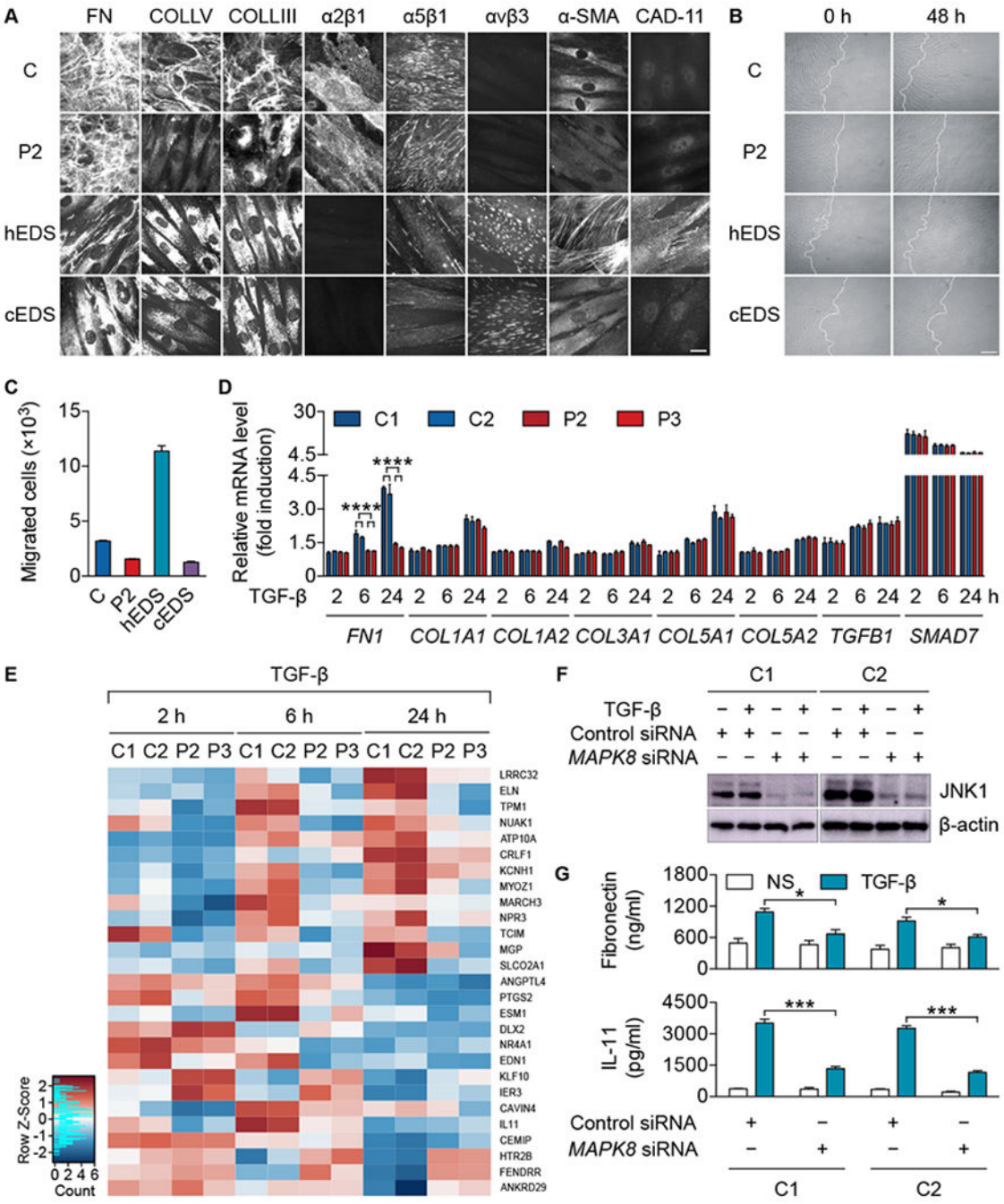

Fig. 5. Impaired response to TGF-β in the patients' fibroblasts.

(**A**) Immunofluorescence of fibronectin (FN), type V collagen (COLLV), type III collagen (COLLIII), α2β1, α5β1, and αvβ3 integrins, α-smooth muscle actin (α-SMA), and cadherin-11 (CAD-11) in primary fibroblasts from a healthy control (C), P2, a patient with hEDS (hEDS) (56), and a patient with cEDS (cEDS) (93). Scale bar: 10 μm. (**B**) *In vitro* scratch assay with primary fibroblasts from a healthy control (C), P2, a patient with hEDS (hEDS) (56), and a patient with cEDS (cEDS) (93). Images were captured at 0 and 48 h after scratching. Scale bar: 100 μm. (**C**) Transwell assay with primary fibroblasts from a healthy

control (C), P2, a patient with hEDS (hEDS) (56), and a patient with cEDS (cEDS) (93). (**D**) mRNA induction in primary fibroblasts from healthy controls (C1 and C2) and patients (P2 and P3) stimulated with TGF-β (10 ng/mL) for the indicated times. (**E**) The top 10 upregulated or downregulated genes in terms of absolute fold change, in primary fibroblasts from healthy controls (C1 and C2) stimulated with TGF-β (10 ng/mL) for 2, 6, and 24 h, with a greater than 1.5-fold change relative to patients (P2 and P3) at each time point. (**F** and **G**) Expression of JNK1 protein (**F**) and production of fibronectin (top panel) and IL-11 (bottom panel) (**G**) by primary fibroblasts from healthy controls (C1 and C2) transfected with control siRNA (50 nM) or *MAPK8* siRNA (50 nM) for 48 h and then stimulated with TGF-β (10 ng/mL) for an additional 24 h. NS, non-stimulated conditions. The values shown are the means ± SEM of two (**C**) or three (**D** and **G**) independent experiments. *, $P < 0.05$, ***, $P < 0.001$, and ****, $P < 0.0001$; in unpaired *t* tests (**D** and **G**).

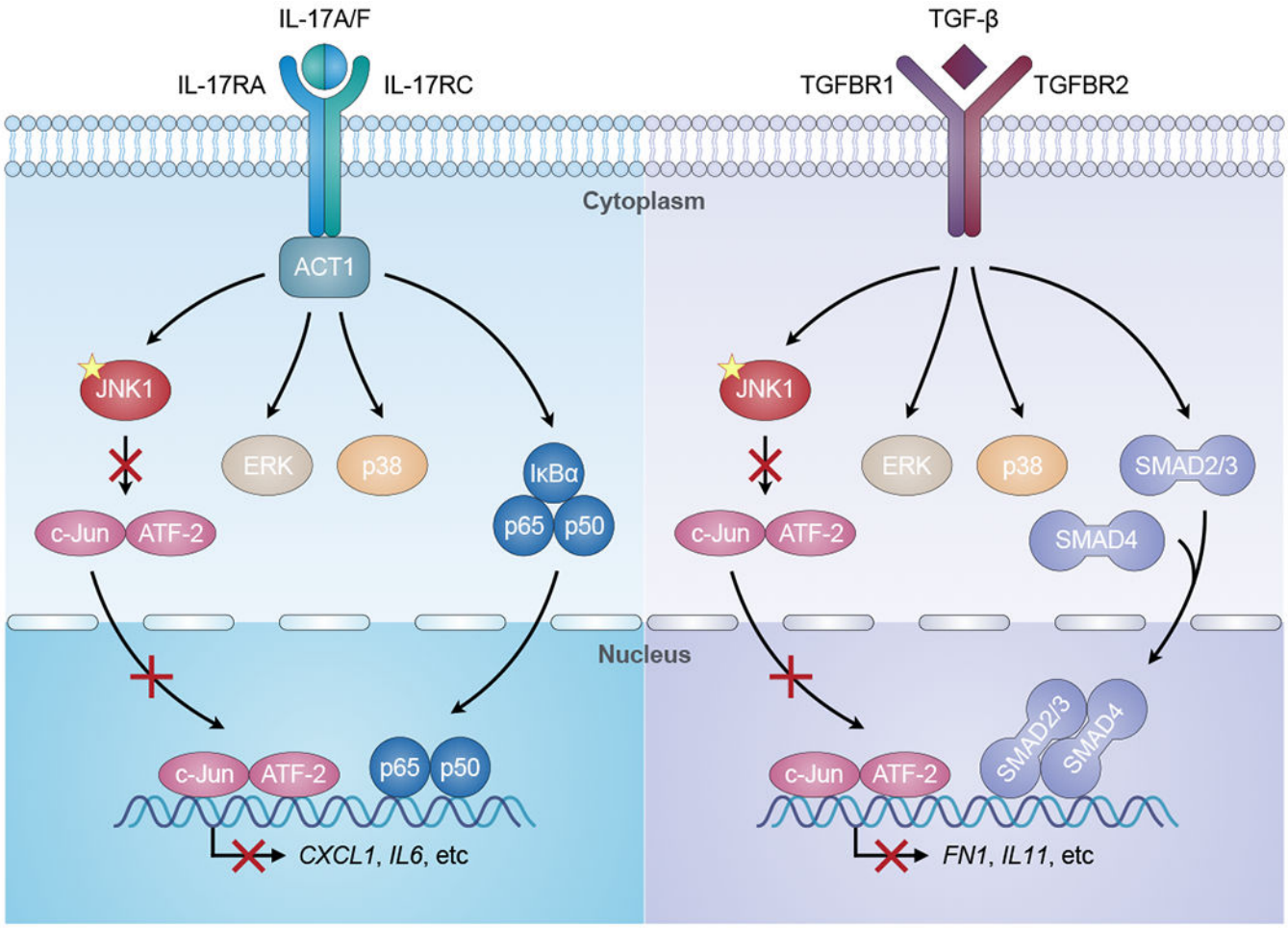

Fig. 6. JNK1-dependent IL-17 and TGF-β signaling.

The binding of IL-17A/F to the IL-17RA/IL-17RC receptor facilitates the recruitment of ACT1 to the receptor, which mediates the activation of JNK1, ERK, p38, and NF-κB (p65/p50) signaling, leading to the production of pro-inflammatory cytokines and chemokines (e.g. *CXCL1*, *IL6*). Similarly, TGF-β binds to its receptor (TGFBR1/TGFBR2), leading to the activation of JNK1, ERK, p38, and SMAD (SMAD2/3/4) signaling. This pathway ultimately results in the production of extracellular matrix proteins and regulators (e.g. *FN1*, *IL11*). The mutation (yellow star) in *JNK1* impairs the JNK1-dependent activation of downstream AP-1 (c-Jun/ATF-2), thereby reducing the JNK1-dependent cellular responses to IL-17 and TGF-β.